Int J Earth Sci (Geol Rundsch) (2009) 98:1221–1238
DOI 10.1007/s00531-008-0370-8

ORIGINAL PAPER

Tectonic evolution of the South Tianshan orogen and adjacent regions, NW China: geochemical and age constraints of granitoid rocks

Jun Gao · Lingli Long · Reiner Klemd · Qing Qian · Dunyi Liu · Xianming Xiong · Wen Su · Wei Liu · Yitian Wang · Fuqun Yang

Received: 26 November 2007 / Accepted: 20 September 2008 / Published online: 16 October 2008

Abstract Geochemical and geochronological evidence was obtained from granitoids of the South Tianshan orogen and adjacent regions, which consist of three individual tectonic domains, the Kazakhstan–Yili plate, the Central Tianshan Terrane and the Tarim plate from north to south. The Central Tianshan Terrane is structurally bounded by the Early Paleozoic 'Nikolaev Line–North Nalati Fault' and Late Paleozoic 'Atbashy–Inyl'chek–South Nalati–Qawabulak Fault' zones against the Kazakhstan–Yili and Tarim plates, respectively. The meta-aluminous to weakly peraluminous granitic rocks, which are exposed along the Kekesu River and the Bikai River across the Central Tianshan Terrane, have a tholeiitic, calc-alkaline or high-potassium calc-alkaline composition (I-type). Geochemical trace element characteristics and the Y versus Rb–Nb or Y versus Nb discrimination diagrams favor a continental arc setting for these granitoid rocks. SHRIMP U–Pb and LA-ICP-MS U–Pb zircon age data indicate that the magmatism started at about 480 Ma, continued from 460 to 330 Ma and ended at about 275 Ma. The earlier magmatism (>470 Ma) is considered to be the result of a simultaneous southward and northward subduction of the Terskey Ocean beneath the northern margin of the Tarim plate and the Kazakhstan–Yili plate, respectively. The later magmatism (460–330 Ma) is related to the northward subduction of the South Tianshan Ocean beneath the southern margin of the Kazakhstan–Yili–Central Tianshan plate. The dataset presented here in conjunction with previously published data support a Late Paleozoic tectonic evolution of the South Tianshan orogen, not a Triassic one, as recently suggested by SHRIMP U–Pb zircon dating for eclogites.

Keywords South Tianshan · Granitoids · SHRIMP and LA-ICP-MS zircon geochronology · Tectonic evolution

Electronic supplementary material The online version of this article (doi:10.1007/s00531-008-0370-8) contains supplementary material, which is available to authorized users.

J. Gao (✉) · Q. Qian · W. Su · W. Liu
Key Laboratory of Mineral Resources, Institute of Geology and Geophysics, Chinese Academy of Sciences, PO Box 9825, 100029 Beijing, China
e-mail: gaojun@mail.igcas.ac.cn

L. Long
Beijing Institute of Geology for Mineral Resources, 100012 Beijing, China

R. Klemd
GeoForschungszentrum Nordbayern, Universität Erlangen, Schlossgarten 5, 91054 Erlangen, Germany
e-mail: klemd@geol.uni-erlangen.de

D. Liu
Beijing SHRIMP Center, Chinese Academy of Geological Sciences, 100037 Beijing, China

X. Xiong
College of Resources and Environmental Engineer, Guizhou University, 550003 Guiyang, China

Y. Wang · F. Yang
Institute of Mineral Resources, Chinese Academy of Geological Sciences, 100037 Beijing, China

Introduction

Considerable continental growth in the Phanerozoic eon has been advocated for the Central Asian orogenic belt (CAOB; Zonenshain et al. 1990), also known as Altaid Tectonic Collage (Altaids; Sengör et al. 1993), which is sandwiched between the Siberian and Sino-Korean–Tarim–

Karakum cratons (Fig. 1a). The evolution of the CAOB is interpreted to be a consequence of lateral accretion of young arc complexes and old terranes (microcontinents) and vertical underplating of mantle-derived magma (Jahn et al. 2000a, b; Jahn 2004; Gao et al. 2002; Chen and Jahn 2004; Li et al. 2006; Kröner et al. 2007, 2008; Windley et al. 2007). Although arc accretion appears to have been the dominant process in the CAOB, postcollisional mantle-derived magmatic intrusions may also have been involved (Han et al. 1997; Zhao et al. 2000; Jahn 2004; Zhou et al. 2004). The southern Tianshan range, which extends west–east for about 2,500 km from Uzbekistan, Tajikistan, Kyrgyzstan, Kazakhstan to Xinjiang in northwestern China, is situated along the southwest margin of the CAOB (Fig. 1a) and marks the final collision between the Tarim and Siberian cratons (Sengör et al. 1993). Thus, its tectonic history plays a very important role to understand both the amalgamation of Eurasia and Phanerozoic continental growth of the CAOB.

The South Tianshan orogen has traditionally been considered to be a Hercynian (Burtman 1975; Khain 1985) or polycyclic Caledonian–Hercynian orogenic belt (Huang et al. 1987; Wang et al. 1990). Windley et al. (1990) proposed a Paleozoic collisional origin for the Yili–Central Tianshan and Tarim blocks, which was reactivated during the Cenozoic. The unroofing of the ancestral Tianshan is documented at the beginning of the Oligocene–Miocene (Hendrix et al. 1994; Yin et al. 1998). However, no consensus has been reached on the timing of the collision of the Yili–Central Tianshan and Tarim blocks and formation of the South Tianshan orogen. The collision is thought to have occurred during the Late Devonian (Xiao et al. 1992; Che et al. 1994; Wang et al. 1994; Xia et al. 2004), Late Devonian–Early Carboniferous (Allen et al. 1992), Early–middle Carboniferous (Coleman 1989; Gao et al. 1998; Zhou et al. 2001; Gao and Klemd 2003) and at the end of Carboniferous to Early Permian (Zonenshain et al. 1990; Shi et al. 1994; Chen et al. 1999a; Heubeck 2001; Bazhenov et al. 2003; Xiao et al. 2004; 2006; Klemd et al. 2005; Gao et al. 2006; Li et al. 2006; Charvet et al. 2007; Solomovich 2007; Konopelko et al. 2007; Wang et al. 2007a; Li et al. 2008).

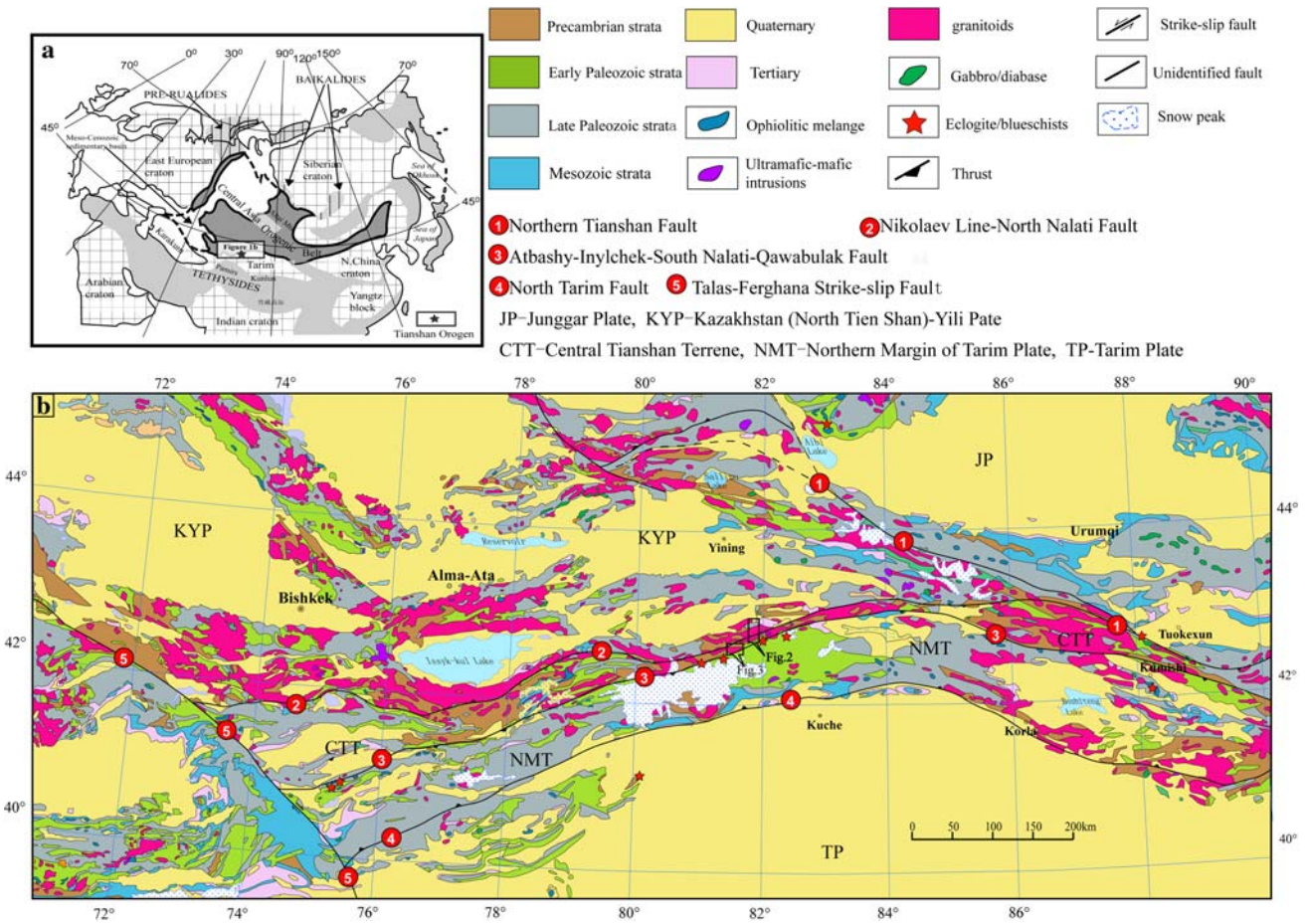

Fig. 1 Tectonic sketch map of the Central Asia orogenic belt (**a**; modified after Yakubchuk 2004) and the geological map of the South Tianshan orogen and adjacent region [**b**; modified after Institute of Geology of Chinese Academy of Geological Sciences (IGCAGS) 2006]

More recently, it was also suggested that the collision for the South Tianshan orogenic belt in Uzbekistan–Tajikistan–Kyrgyzstan (Brookfield 2000) and NW China (Li et al. 2002, 2005a; Zhang et al. 2005a, 2007a, b; Xiao et al. 2008) occurred during the Triassic.

In this paper, we present new geochemical and geochronological data from granitoid rocks in the Chinese part of the South Tianshan orogen and adjacent regions. Furthermore, we discuss the tectonic evolution of the South Tianshan orogen and the timing of the collision between the Tarim and Kazakhstan–Yili blocks to establish a geotectonic framework of Paleozoic Central Asia.

Regional geology

In China, the Tianshan Mountains are divided into two segments, the Eastern Tianshan and the Western Tianshan along Tuokexun–Kumishi High Road (Ma et al. 1993, 1997). The Western Tianshan is divided further into the 'South Tianshan,' 'Central Tianshan' and 'North Tianshan' (Huang et al. 1987; Wang et al. 1990; Allen et al. 1992). The Yili block is part of the Central Tianshan according to this scheme. Additionally, the South Tianshan orogen was interpreted as collisional belt between the Central Tianshan (including Yili block) and Tarim blocks (Windley et al. 1990; Allen et al. 1992; Gao et al. 1998). However, the 'Tien Shan' as described in Russia, Kyrgyzstan, Kazakhstan and Uzbekistan is usually divided into three subunits from the south to north, the 'South Tien Shan' Hercynian fold system, the 'Middle Tien Shan' Massif and the 'Northern Tien Shan' Massif, the southern margin of which is superimposed by Caledonian granites and Devonian–Carboniferous volcanics in Kyrgyzstan (Khain 1985; Zonenshain et al. 1990; Bazhenov et al. 2003). The 'Northern Tien Shan' Massif was traditionally regarded to be part of the Kazakhstan–Yili plate (Li et al. 1982). To obliterate the rift between the Former Soviet and Chinese literature, we have compared these terms and their characteristics in detail and propose a scheme for the subdivision of the Tianshan across the border area (Qian et al. 2008). The South Tianshan orogen and adjacent regions can be subdivided into three distinct tectonic domains, the Kazakhstan (North Tien Shan)–Yili plate, the Central Tianshan Terrane and the Tarim plate (Fig. 1b; Zonenshain et al. 1990; He and Li 2000; He et al. 2001; Qian et al. 2008).

The Kazakhstan–Yili plate (also known as the North Tien Shan–Yili plate) is separated from the Central Tianshan Terrane by the 'Nikolaev Line' in Kyrgyzstan and Kazakhstan and the 'North Nalati Fault' in Xinjiang in northwestern China (Fig. 1b; Khain 1985; Lomize et al. 1997; Li and Li 1997; He et al. 2001; Qian et al. 2008). In the Yili block of NW China, Precambrian granitic gneisses with a U–Pb zircon age of 798 Ma and Sm–Nd model ages varying from 1.93 to 2.01 Ga (Chen et al. 1999b) are covered unconformably by Meso–Neoproterozoic carbonates, clastic rocks and minor tillites, together with the Cambrian–Early Ordovician siltstones, mudstones, sandstones and volcanics (Gao et al. 1998). Furthermore, granites [471 Ma, titanite U–Pb age; Bureau of Geology and Mineral Resources of Xinjiang Uygur Autonomous Region (BGMXJ) 1993] and diorites (470 ± 12 Ma, SHRIMP U–Pb zircon age) intruded the Paleozoic volcanics (Qian et al. 2008). Early Carboniferous andesites, basaltic andesites and basalts have an U–Pb zircon age of 363 ± 6 Ma (Zhai et al. 2006) and $^{40}Ar/^{39}Ar$ plateau ages of 334–360 Ma (Liu et al. 1994); Late Carboniferous–Early Permian alkali–rich volcanic rocks including shoshonites and alkaline porphyries (Zhao et al. 2000; 2003) are distributed extensively along the southern margin of the Yili block. In the southern part of the Kazakhstan block (also known as the Northern Tien Shan in Kyrgyzstan), Archean granitic gneisses with a U–Pb SHRIMP zircon age of 2,791 ± 24 Ma and Paleoproterozoic granitic gneisses with ages of 2,187 and 1,789 Ma are exposed in southern Kazakhstan (Kröner et al. 2007). Furthermore, Cambrian to Lower Arenigian (earliest Early Ordovician) oceanic and island arc complexes were thrusted over the Precambrian basement (Mikolaichuk et al. 1997). Middle Arenigian conglomerates and olistostromes unconformably overlie these complexes. Precambrian to Middle Ordovician rocks are intruded by granites of middle Ordovician age (464 Ma, zircon U–Pb, Kiselev 1999; 460–470 Ma, zircon U–Pb, Konopelko et al. 2008) and Early Silurian (435–440 Ma, zircon U–Pb, Konopelko et al. 2008). Upper Arenigian to Lower Caradocian volcanics of island–arc affinity and Upper Ordovician redbeds are unconformably covered by Devonian volcanics, Lower Carboniferous redbeds, and Upper Carboniferous conglomerates and sandstones (Mikolaichuk et al. 1995). Permian alkali-rich volcanic rocks including shoshonites unconformably overlie Upper Carboniferous sedimentary rocks (Solomovich 2007). K–Ar ages of shoshonitic/ultrapotassic volcanics lie in the range of 296–268 Ma (Ges et al. 1982).

Ophiolites are exposed along the 'Nikolaev Line' and its eastern extension, the 'North Nalati Fault,' either as autochthous or as allochthonous blocks, which were thrusted over the early Paleozoic island–arc complexes in the northern Tien Shan of Kyrgyzstan (Bazhenov et al. 2003; Qian et al. 2008). They are interpreted as relics of a paleo-ocean called the 'Kyrgyz–Terskey Ocean,' which is supposed to have formed from the end of Riphean (latest Neo-Proterozoic) until middle Early Ordovician (Lomize et al. 1997). Mid-oceanic ridge basalts with a SHRIMP U–Pb zircon age of 516 ± 7 Ma have been reported to occur

along the southern margin of the Yili block (Qian et al. 2008). To the east, the Nicolaev Line is terminated by the Northern Central Tianshan Suture (Guo et al. 1993; Gao et al. 1998; Qian et al. 2008). Paragonite from the Makbal eclogites, which are exposed at the western termination of this suture zone, has a K–Ar age of 482 ± 17 Ma (Tagiri et al. 1995).

The Central Tianshan Terrane is separated from the northern margin of the Tarim plate along the Southern Central Tianshan Suture (SCTS; also known as the Atbashy–Inyl'chek Fault in Kyrgyzstan and South Nalati–Qawabulak Fault in NW China; Fig. 1b). It is underlain by Meso- to Neoproterozoic metamorphic basement, composed of sillimanite–biotite–quartz schists, garnet–plagioclase–granulites, gneisses, amphibolites, migmatites and marbles (Xiao et al. 1992; Che et al. 1994; Milanovsky 1996; Li and Li 1997). The basement is unconformably overlain by Sinian carbonates and tillites. Granulites with a U–Pb zircon age of 1,910 Ma [Liao Ning Institute of Geological Survey (LNIGS) 2005] and granitic gneisses with a U–Pb zircon age of 882 ± 33 Ma and a Sm–Nd model age of 2.65 Ga (Chen et al. 2000b) were identified in the basement. Cambrian–Ordovician rocks are made up of carbonates and flysch in Kyrgyzstan (Milanovsky 1996), but are absent in the Chinese segment. Late Silurian island–arc type volcanics and volcaniclastic rocks were thrusted directly over the Precambrian metamorphic rocks (Gao et al. 1998). Furthermore, Carboniferous island–arc type volcanics and volcaniclastic rocks with SHRIMP U–Pb zircon ages of 354 and 313 Ma disconformably lie on Late Silurian volcanics or Precambrian basement (Zhu et al. 2005). Inherited zircons with $^{206}Pb/^{238}U$ ages between 2,478 and 2,567 Ma have also been found in the Carboniferous basalts (Zhu et al. 2006a). Late Permian neritic carbonates, clastic rocks or continental sandstones, pelites, and conglomerates are also present locally. Early Paleozoic to Late Paleozoic diorites and granites with zircon U–Pb ages varying from 457 to 266 Ma (Han et al. 2004; Yang et al. 2006; Zhu et al. 2006b; Gao et al. 2006) are extensively exposed in the Central Tianshan Terrane.

As already pointed out, the SCTS represents a Late Paleozoic suture between the Central Tianshan and Tarim plates (Windley et al. 1990; Allen et al. 1992; Tagiri et al. 1995; Gao et al. 1998; Solomovich 2007; Konopelko et al. 2007; Qian et al. 2008). Paleozoic ophiolitic mélanges (Gao et al. 2006) and two typical high-pressure/low-temperature metamorphic (HP–LT) terranes, the Atbashy terrane in Kyrgyzstan and South Tianshan (also known as western Tianshan) terrane in NW China are exposed along this suture zone (Fig. 1b). The former is composed mainly of greenschist-facies and blueschist-facies meta–pelitic to siliceous schists alternating with bluechists and eclogites (Dobretsov et al. 1987; Tagiri et al. 1995). The blueschists have K–Ar whole rock ages of 410–350 Ma (Dobretsov et al. 1987) and a K–Ar glaucophane age of 360 ± 10 Ma (Zamaletdinov 1994). In addition, the Atbashy eclogites have a Rb–Sr isochron age of 267 ± 5 Ma (wr–grt–omp–ph1–ph2; Tagiri et al. 1995) and $^{40}Ar/^{39}Ar$ plateau ages of 327–324 Ma for phengites (Stupakov et al. 2004). The South Tianshan HP–LT terrane is mainly composed of blueschist-, eclogite- and greenschist-facies metasedimentary rocks and some mafic metavolcanic rocks with N-MORB, E-MORB and OIB affinities (Gao et al. 1999; Gao and Klemd 2003; Ai et al. 2005; Li et al. 2007). Blueschists occur within greenschist-facies metasediments as small discrete bodies, lenses, bands and thick layers. Eclogites are interlayered with the blueschist layers as pods, boudins, thin layers or as massive blocks. The transition between blueschist and eclogite is locally gradual, and both underwent prograde metamorphic conditions of 480–580°C at 1.9–2.1 GPa (e.g., Klemd et al. 2002; Wei et al. 2003; Lin and Enami 2006). UHP-conditions for some eclogites were reported and discussed (cf. Zhang et al. 2002a, b, 2003, 2005b; Klemd 2003). Networks of eclogite-facies veins derived from the dehydration of blueschists are widely present in the HP–LT metamorphic terrane (Gao and Klemd 2001; Gao et al. 2007; John et al. 2008). A Sm–Nd isochron age (omp–gln–grt–wr) of 343 ± 44 Ma and well-defined $^{40}Ar/^{39}Ar$ ages of 344 ± 1 and 345 ± 1 Ma for glaucophane suggest a Carboniferous age for the peak of metamorphism (Gao and Klemd 2003; Gao et al. 2006). White mica geochronology (K–Ar, Ar–Ar, Rb–Sr) supplies ages varying from 335 to 310 Ma, interpreted to date exhumation (Klemd et al. 2005). $^{40}Ar/^{39}Ar$ plateau ages varying from 415 to 350 Ma have also been previously obtained for glaucophane and mica of blueschists (Xiao et al. 1992; Gao et al. 1995, 2000). In contrast, zircon from eclogites yields SHRIMP U–Pb core ages of 413–310 Ma and rim ages of 266–226 Ma, of which the latter were interpreted to represent the timing of peak metamorphic conditions (Zhang et al. 2007a, b). Close to the eastern termination of the SCTS, high-pressure granulite exotic blocks (Shu et al. 1999; 2004) and relic blueschists have been found in the matrix of ophiolitic mélanges (Fig. 1b; Gao et al. 1993). A peak metamorphic age of 364 ± 5 Ma (Wang et al. 1998) and a $^{40}Ar/^{39}Ar$ plateau age of 360 ± 2 Ma (Liu and Qian 2003) were obtained for the granulites and blueschists, respectively.

The northern margin of the Tarim plate is composed of Proterozoic metamorphic rocks, Sinian shallow marine clastic rocks, carbonates, tillites, Lower Cambrian black shales and phosphoric silicates, Cambrian–Carboniferous marine/nonmarine carbonates, clastic rocks, cherts and interlayered volcanics (Allen et al. 1992; Carroll et al. 1995). Permian fluvial deposits and rift-type volcanics

unconformably overlie the earlier strata (Carroll et al. 1995). Granitic gneisses with a U–Pb zircon age of 707 ± 13 Ma and a Sm–Nd model age of 1.9 Ga (Chen et al. 2000a) and blueschist-facies meta-pelites with Rb–Sr isochron and K–Ar ages of about 700 Ma (Nakajima et al. 1990) are exposed in the northwestern margin of the Tarim basin. Granulite xenoliths from the Cretaceous Tuoyun basalts exhibit LA-ICPMS U–Pb zircon ages of 690–770 Ma and Hf model ages of 1.3–1.7 Ga (Zheng et al. 2006a, b). Silurian–Early Carboniferous ophiolitic klippes were thrusted over the Paleozoic sedimentary strata (Gao et al. 1998; Long et al. 2006). Late Devonian–Early Carboniferous radiolarias have been found in cherts, which are constituents of ophiolitic mélanges (Liu 2001; Liu and Hao 2006). Permian syenites, nepheline syenites, aegirine syenites, two-mica peraluminous leucogranites and A-type rapakivi granites extensively intruded into Paleozoic sedimentary strata (Jiang et al. 1999; Solomovich and Trifonov 2002; Liu et al. 2004; Konopelko et al. 2007; Solomovich 2007; Long et al. 2008). A Rb–Sr isochron age of 269 ± 21 Ma (Solomovich and Trifonov 2002) and a U–Pb zircon age of 296 ± 4 Ma (Mao et al. 2004) were obtained for the Jangart rapakivi granite and rapakivi quartz syenite in Kokshaal. Recently, Konopelko et al. (2007) reported new U–Pb zircon ages of 297 ± 4 Ma for the Jangart granite, 279 ± 8 Ma for the Uch–Koshkon granite, 281 ± 2 Ma for the Mudryum granite and 279 ± 3 Ma for the Kok–Kiya granite. U–Pb zircon ages of 279–273 Ma were obtained for nepheline and aegirine syenites in the Chinese Haerkeshan (Liu et al. 2004). Additionally, some granites with zircon ages varying from 490 to 435 Ma were also reported to occur in the eastern segment of the South Tianshan (Hopson et al. 1989; Han et al. 2004).

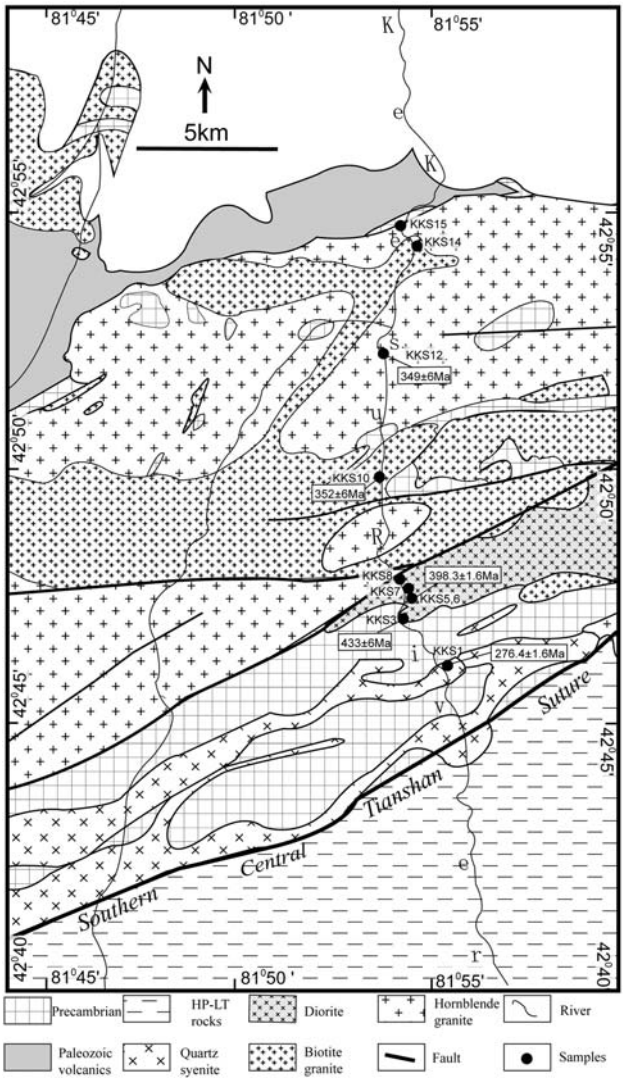

Fig. 2 Geological map showing the sample localities along Kekesu River across the Central Tianshan Terrane (modified after Long 2007)

Localities and Petrology

Granitic rocks exposed along the Kekesu river and the Bikai river across the Central Tianshan Terrane (Figs. 1b, 2, 3) were selected for geochemical and geochronological investigations. Various types of granitic rocks are exposed along the Kekesu river profile (Fig. 2). Along the southern segment of the profile, a quartz syenite pluton intrudes into Meso- to Neoproterozoic sillimanite–biotite–quartz schists, garnet–plagioclase–granulites, gneisses, amphibolites and marbles and Paleozoic greenschists, which are components of the 'Western Tianshan subduction complex' (Gao et al. 1995; Gao and Klemd 2003). Sample KKS1 is composed of microperthite (50%), plagioclase (20%), quartz (20%), biotite (5%) and some accessory minerals such as zircon, apatite, ilmenite and titanite. To the north, a composite dioritic pluton, which is made up of diorite, hornblende granite and monzodiorite, also intruded into Meso- to Neoproterozoic metamorphic rocks and has itself been intruded by a biotite granite. In places, a gneissic texture was observed indicating a postemplacement metamorphic overprint. The diorite sample (KKS6/7/8) contains plagioclase (60%), hornblende (30%), quartz (5%), chlorite (3%) and some accessory minerals. The hornblende granite sample (KKS3) is composed of hornblende (20%), plagioclase (20%), alkali feldspar (40%) and quartz (20%). The monzodiorite sample (KKS5) contains hornblende (35%), biotite (5%), feldspar (55%) and quartz (5%). The hornblende–biotite granite pluton is intruded by a younger biotite granite along the north segment of the profile. The former (sample KKS12/15) is composed mainly of plagioclase (15%), alkali feldspar (50%), quartz (30%), hornblende (2%), biotite (<1%) and accessory minerals, while the latter (sample KKS10/14) contains plagioclase

(15%), alkali feldspar (45%), quartz (34%), biotite (1%) and accessory minerals such as zircon, apatite, ilmenite and magnetite. Both the hornblende–biotite granite and the biotite granite are intrusive into Lower Carboniferous country rocks.

A composite granitic intrusion comprising granite and granodiorite is exposed along the Bikai river (Fig. 3). It intrudes into Meso- to Neoproterozoic amphibole–biotite–plagioclase schists, garnet–plagioclase–granulites, gneisses and amphibolites and is overlain by the western Tianshan HP–LT metamorphic belt, which is mainly composed of blueschist-, eclogite- and greenschist-facies meta-sedimentary rocks and some mafic metavolcanic rocks (Gao et al. 1995, 1999; Gao and Klemd 2003). The granite (samples BK6-1/7/12-1/13/14) displays a gneissic foliation, which is parallel to the main ENE regional trend. It comprises plagioclase (20%), alkali feldspar (25%), quartz (45%), biotite (10%) and accessory minerals such as zircon, apatite, ilmenite and magnetite. However, the granodiorite (samples BK4/10/15) displays a massive texture, and contains plagioclase (40–60%), quartz (15–40%), hornblende (10–20%), minor chlorite and accessory minerals.

Analytical methods

Major oxides were determined by X-ray fluorescence spectrometry (XRF) on fused glass disks, using a PHILLIPS PW1480, at the Institute of Geology and Geophysics of the Chinese Academy of Sciences (IGGCAS). Uncertainties for most major oxides are <2%, for MnO and P_2O_5 <5% and totals are within 100 ± 1%. Loss on ignition (LOI) was measured after heating to 1,000°C. Trace element concentrations were analyzed by inductively coupled plasma mass spectrometry (ICP-MS; Finnigan Element) at the IGGCAS. The detailed analytical procedure is identical to that used by Qian et al. (2006, 2008). Relative standard deviations (RSD) are within ±10% for most trace elements but reach ±20% for V, Cr, Co, Ni, Th and U according to analysis of rock standards.

The in situ laser ablation (LA)-ICPMS zircon dating was done at the Key Laboratory of Continental Dynamics of the Northwest University of China. The hand-picked zircons were mounted onto epoxy resin discs and polished to expose the grain centers. Cathodoluminescence (CL) images were taken by a Cameca SX-51 Electron Microscope at IGGCAS. The analytical voltage and current was 50 kV and 15 nA, respectively. The ICP-MS used in this study is an ELAN6100 from Perkin Elmer/SCIEX (ON, Canada) with a dynamic reaction cell (DCR). The GeoLas 200M laser-ablation system (MicroLas, Gottingen, Germany) was used for the laser ablation experiments. The system is equipped with a 193 nm ArF-excimer laser from Lambda Physik. The ablation spot size was about 30 μm. Helium was used as the carrier gas to enhance the transport efficiency of the ablated material. The detailed experimental procedure was the same as that reported by Yuan et al. (2003). All measurements were performed using the zircon standard 91500 as external standard for the age calculation

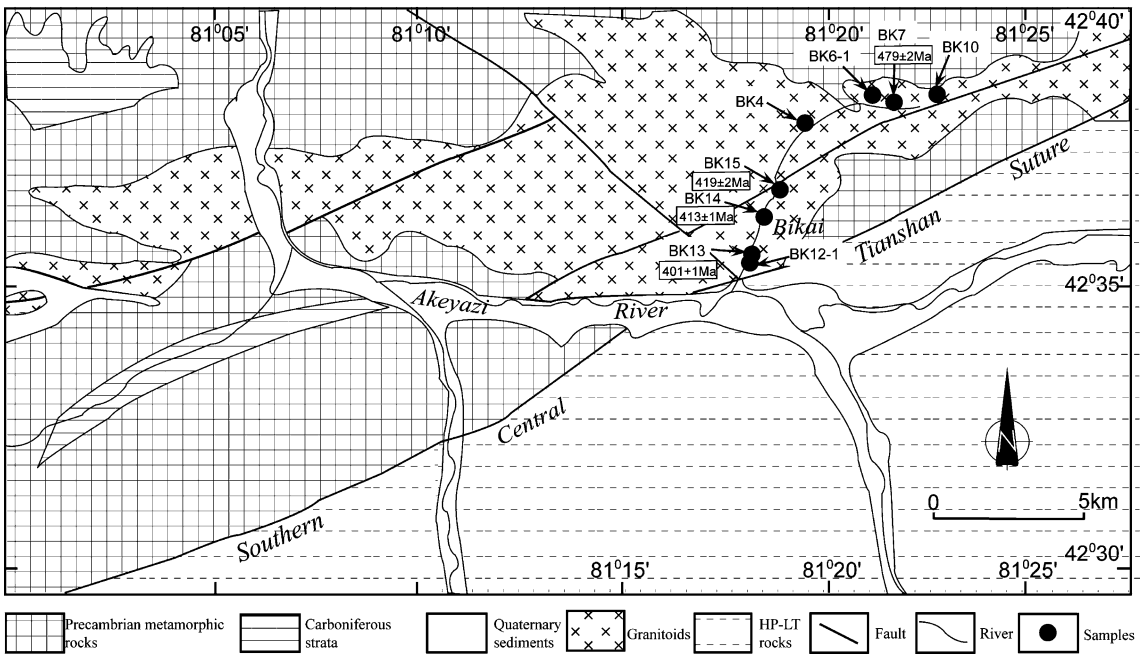

Fig. 3 Geological map showing the sample localities along the Bikai River across the Central Tianshan Terrane (modified after Long 2007)

(Wiedenbeck et al. 1995) and NIST SRM 610 as external standard for the concentration calculation in conjunction with the internal standardization using ^{29}Si (32.8% SiO_2 in zircon). Isotopic ratios and elemental concentrations were calculated using GLITTER 4.0 (Macquarie University), while Isoplot (version 2.0; Ludwig 1991) was used for the age calculation and plotting of concordia diagrams.

The SHRIMP (Sensitive High Resolution Ion Microprobe) analyses were performed on the SHRIMP II instrument at the Beijing SHRIMP Center of the Chinese Academy of Geological Sciences (CAGS). Zircons were selected from the crushed rocks by a combination of heavy liquid and magnetic separation techniques. Individual crystals were mounted in epoxy resin discs together with pieces of the Canberra standard TEMORA (417 Ma; Black et al. 2003). The discs were polished and zircons were half-sectioned, followed by cleaning and gold-coating. Cathodoluminescence (CL) images were taken by the Hitachi S-3000N Scanning Electron Microscope at CAGS. Spot sizes for the SHRIMP analyses averaged 30 μm and mass resolution at about 5,000 for measuring Pb/Pb and Pb/U isotopic ratios. The ^{238}U concentrations were normalized to the standard SL13 (^{238}U = 238 ppm; age: 572 Ma). The analyses of standard TEMORA and samples were alternated (1:3) for correcting Pb^+/U^+ discrimination. The data reported in Electronic Supplementary Material Table 2 are corrected by assuming $^{206}Pb/^{238}U$–$^{208}Pb/^{232}Th$ age-concordance. The SQUID (Version 1.03d) and ISOPLOT (Version 3.00) programs of K.R. Ludwig were used to process the data.

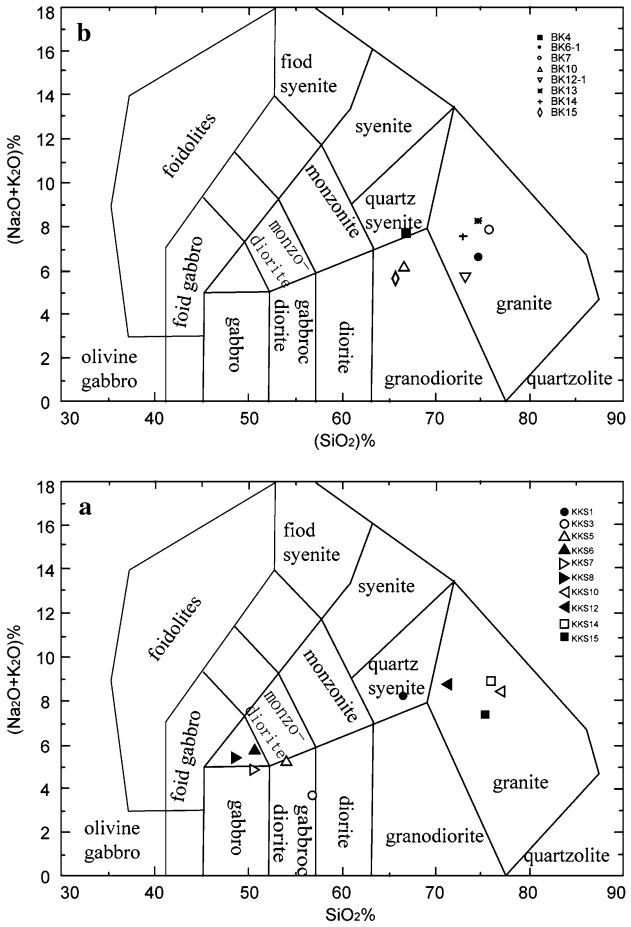

Fig. 4 TAS classification diagram (after Middlemost 1994) of the granitoids from Kekesu River (**a**) and Bikai River (**b**)

Results

Geochemical characteristics

Major, trace and rare earth elements of representative granitic rocks are given in the Electronic Supplementary Material Table 1. Major and trace elements for two geological profiles are presented separately.

Kekesu River profile

Sample KKS1 from the quartz syenite pluton classifies as quartz syenite when using the classification of Middlemost (1994, Fig. 4a). The rock plots in the high-potassium calc-alkaline field in the K_2O–SiO_2 diagram (Fig. 5a) of Peccerillo and Taylor (1976). The syenite is meta-aluminous (A/CNK is 0.75, Fig. 5b, after Maniar and Piccoli 1989) and has a K_2O/Na_2O ratio of 1.01. The chondrite-normalized rare earth element pattern is characterized by moderate enrichment in light REEs, flat heavy REEs and a negative Eu anomaly (Fig. 6a). The primitive mantle (PM)-normalized spidergram shows negative anomalies for Ba, Sr, Nb, Ta and Ti (Fig. 6b).

The dioritic intrusion comprises diorite, monzodiorite and gabbro diorite (Fig. 4a). The K_2O–SiO_2 diagram displays a tholeiitic affinity for all samples (Fig. 5a). K_2O/Na_2O ratios vary from 0.14 to 0.34 and A/CNK from 0.67 to 0.85 (Fig. 5b), indicating a meta-aluminous character of these rocks. The total REE concentrations of these different rock types show large variations from 39.1 to 213 ppm. The diorite sample displays a weak positive Eu anomaly, while the monzodiorite and hornblende granite have distinct negative Eu anomalies (Fig. 6a). The diorite and hornblende granites display relative depletions of Nb and Ti and enrichments of Ba and Sr, whereas the Monzodiorite shows no Nb depletion in the PM-normalized spidergram (Fig. 6b).

K_2O/Na_2O ratios of the hornblende–biotite granite intrusion vary from 0.86 to 1.69, and the samples plot in the transitional calc-alkaline and high-potassium calc-alkaline field of the K_2O–SiO_2 diagram (Fig. 5a). The A/CNK ratio varies from 0.95 to 0.99, indicating the

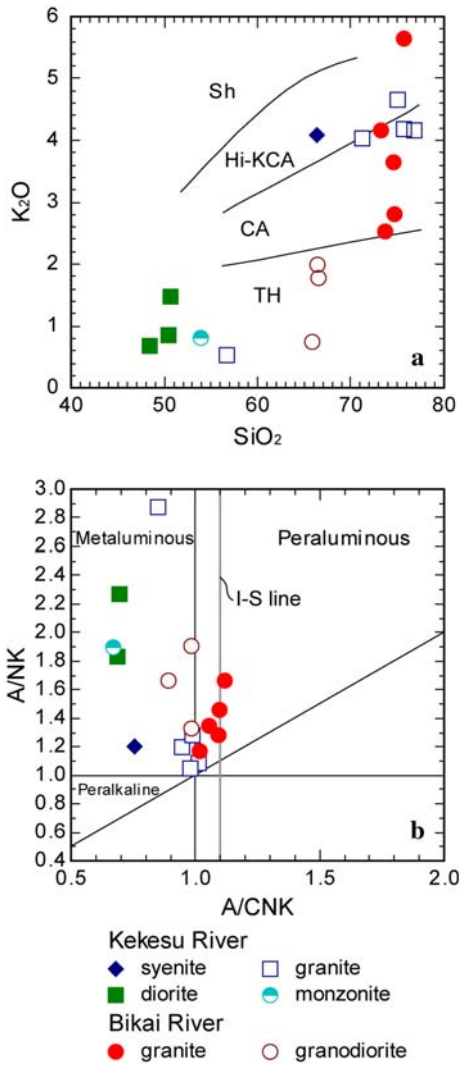

Fig. 5 Major element diagrams for the granitoids. **a** SiO_2 versus K_2O diagram (boundary after Peccerillo and Taylor 1976); **b** A/CNK versus A/NK diagram (Shand's molar parameters in the diagram after Maniar and Piccoli 1989)

meta-aluminous character of all samples (Fig. 5b). K_2O/Na_2O ratios of the samples of the biotite granite intrusion vary from 0.88 to 0.99, while the A/CNK ranges from 0.98 to 1.01 (Fig. 5b), implying that all samples from this pluton are also meta-aluminous and calc-alkaline in character. The REE-element patterns of all samples are similar, with moderate enrichment in light REEs, flat heavy REEs and negative Eu anomalies (Fig. 6c). Furthermore, all samples display negative anomalies in Nb, Ta, P, Sr and Ti in the PM-normalized spidergram (Fig. 6d). In addition, the biotite granite is also depleted in Ba (Fig. 6d).

Bikai River profile

The samples from this granitic pluton are classified as granodiorite and granite (Fig. 4b). The granites plot within the calc-alkaline to high-potassium calc-alkaline fields in the K_2O–SiO_2 diagram (Fig. 5a). The A/CNK varies from 1.02 to 1.21 (Fig. 5b), indicating a weak peraluminous character. The K_2O/Na_2O ratio of the granodiorites varies from 0.15 to 0.47 and plots in the tholeiitic field in the K_2O–SiO_2 diagram (Fig. 5a). The A/CNK varies from 0.89 to 0.98 (Fig. 5b), implying a meta-aluminous character. The granite sample BK10 shows a relative enrichment of Th, U, Zr and Hf without a depletion of Nb when compared with the other samples. The REE patterns of most granite samples are characterized by a moderate enrichment in light REEs, flat heavy REEs and negative Eu anomalies, with σEu $[Eu_N/(Sm_N \times Gd_N)^{0.5}]$ from 0.25 to 0.72 (Fig. 6e), whereas sample BK6-1 has a positive Eu anomaly with a σEu value of 1.46. Most granite samples display negative anomalies of Ba, Sr, Nb, Ta, P and Ti and positive anomalies of Th, La, Ce, Zr and Hf in the primitive mantle (PM)-normalized spidergram (Fig. 6f). Sample BK6-1, however, shows no enrichment of La and Ce and no depletion of Nb and Ta. The REE patterns of the granodiorites are characterized by a moderate enrichment of light REEs, depletion of heavy REEs and positive Eu anomalies (Fig. 6g). The σEu value varies between 1.05 and 2.51. Most samples display negative anomalies of Nb, Ta and Ti and positive anomalies of Ba, Sr and K in the PM-normalized spidergram (Fig. 6h).

U–Pb zircon dating

Zircon grains were separated from nine samples and U–Pb analyses were conducted by means of the SHRIMP (sample KKS 3/10/12) and LA-ICP-MS (KKS1/5, BK7/13/14/15) methods. The analytical results for all nine samples are presented in Electronic Supplementary Material Table 2. Zircon grains are usually elongated or short and prismatic with a grain size varying from 100 to 500 μm. They are colorless to light brown, transparent and euhedral with well-developed concentric oscillatory zoning, indicating a magmatic origin. In the following, the geochronological results for the two geological profiles are presented separately.

Kekesu River profile

Twenty-five spots were analyzed on zircon grains from the quartz syenite (sample KKS1), whereby the results are shown on a concordia plot (Fig. 7a). Eighteen analytical points define a concordant to near-concordant group with a weighted mean $^{206}Pb/^{238}U$ age of 275 ± 3 Ma (Fig. 7a). Three analyses give older ages of 309–333 Ma and two give 401 and 502 Ma, respectively, suggesting that these zircons are possibly xenocrysts. Two analyses give younger ages of 238 and 267 Ma, respectively. Multiple Pb

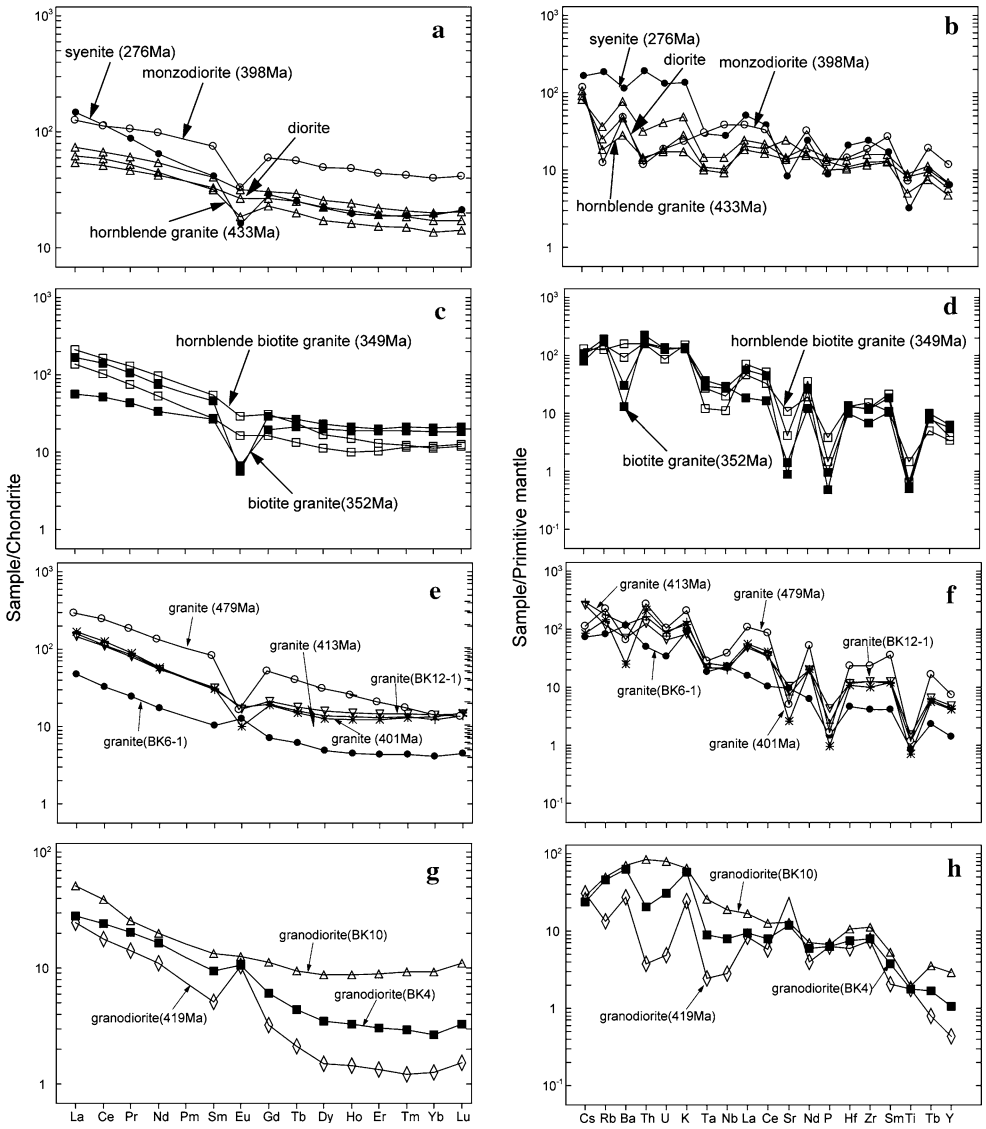

Fig. 6 Rare earth element pattern and spidergrams of the granitoids from Kekesu River and Bikai River (the chondrite REE values from Sun and McDonough 1989 and the primitive mantle-normalized values from Wood et al. 1979)

loss during later-stage thermal or deformational events may account for these younger ages.

All 18 spots analyzed on zircons of the hornblende granite (sample KKS3) cluster on the concordia curve, giving a weighted mean $^{206}Pb/^{238}U$ age of 433 ± 6 Ma (Fig. 7b). Most of the 25 analyzed spots on zircons the monzodiorite sample (KKS5) are concordant, yielding a weighted mean $^{206}Pb/^{238}U$ age of 398 ± 1 Ma (Fig. 7c). Several analyses give older ages ranging between 412 and 438 Ma, indicating that they may stem from inherited zircons. The analysis with a strongly discordant age of 369 Ma may result from Pb loss.

Nineteen spots were analyzed on zircon grains from the biotite granite sample (KKS10). Eighteen points are concordant and give a weighted mean $^{206}Pb/^{238}U$ age of 352 ± 5 Ma (Fig. 7d). Spot 13 with an age of 538 Ma was excluded, since it may stem from an inherited zircon. Fifteen measurements were taken on zircons from the hornblende–biotite granite sample (KKS12). Thirteen concordant zircon analyses yield a weighted mean $^{206}Pb/^{238}U$ age of 349 ± 6 Ma (Fig. 7e). Two spots (3.1/13.1) with older ages (441 and 420 Ma) were excluded from the age calculation.

Bikai River profile

Zircons from three granite samples (BK7/13/14) and one granodiorite sample (BK15) were chosen for U–Pb analyses. Seventeen spots were analyzed on zircons from the sample BK7. Ten concordant analyses give a weighted mean $^{206}Pb/^{238}U$ age of 479 ± 2 Ma (Fig. 7f). The other spots were rejected due to their strong discordance. Twenty-six spots were analyzed on zircon grains from Sample BK13. Eleven analyses are concordant and give a weighted

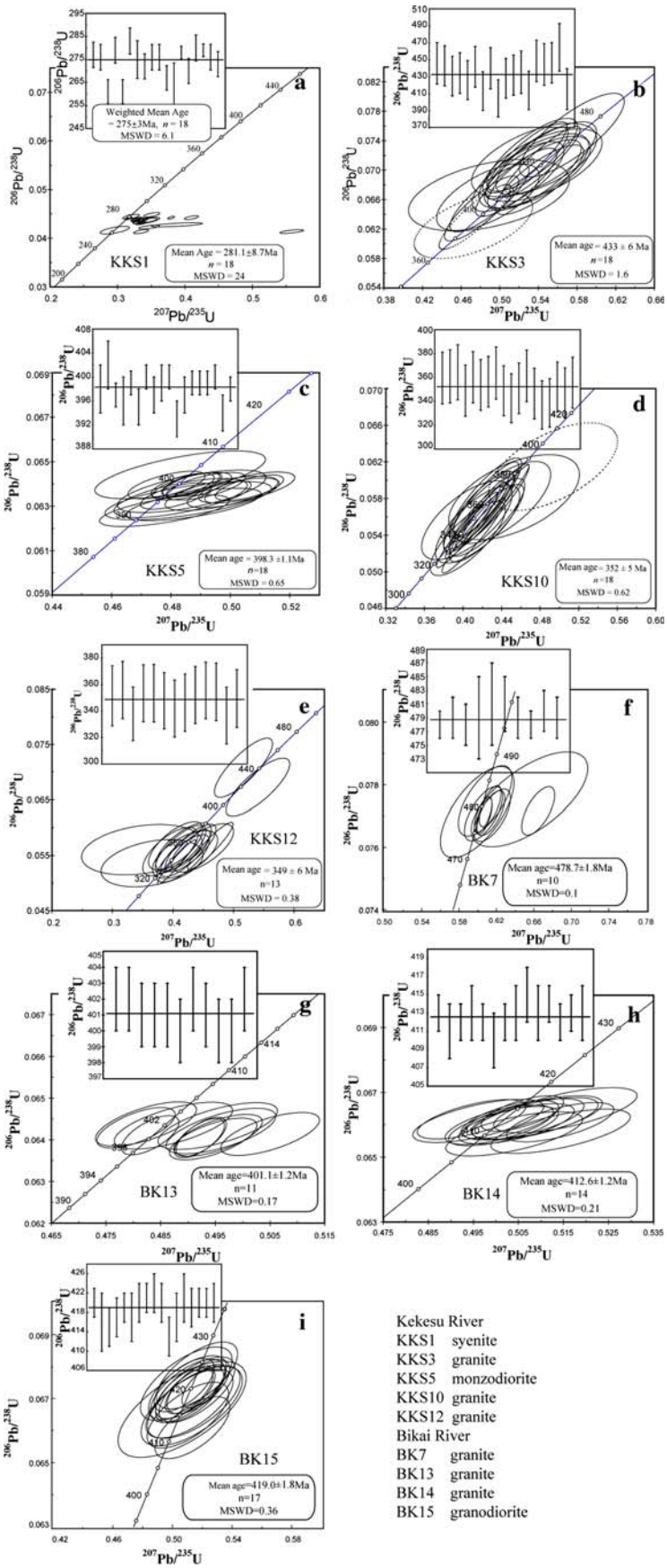

Fig. 7 U–Pb concordia diagrams showing zircon ages obtained by LA-ICPMS and SHRIMP methods

mean $^{206}Pb/^{238}U$ age of 401 ± 1 Ma (Fig. 7g). The other spots are strongly discordant and were thus excluded from the $^{206}Pb/^{238}U$ age calculation. However, some spots (13.11/13.17/13.26) give older ages ranging from 420 to 479 Ma thereby implying the presence of inherited zircons. Twenty-five spots were analyzed for sample BK14. Fourteen concordant analyses yield a weighted mean $^{206}Pb/^{238}U$ age of 413 ± 1 Ma (Fig. 7h). Apart from several discordant analyses, which were excluded from the age calculation, one analysis (14.2) with a concordant age of 1,086 Ma is of particular interest, since it shows the presence of inherited zircons from the Precambrian basement. Twenty-nine spots were analyzed on zircons from Sample BK15. Seventeen concordant analyses yield a weighted mean $^{206}Pb/^{238}U$ age of 419 ± 2 Ma (Fig. 7i).

Discussion

Tectonic setting for the granitoids

The tholeiitic, calc-alkaline or high-potassium calc-alkaline (Fig. 5a) and the meta-aluminous or only weakly peraluminous (Fig. 5b) character of all granitic samples from both the Kekesu River and Bikai River suggest that these rocks stem from an igneous source, i.e., I-type. This interpretation is further supported by the widespread occurrence of hornblende in all granitic rocks, with the exception of the syenite. Furthermore, all granitoids follow the I-type trend as defined by Chappell and White (1992) on the P_2O_5 versus SiO_2 diagram (Fig. 8). In tectonic discrimination diagrams (Pearce et al. 1984) such as Y + Nb versus Rb and Y versus Nb, all granitoids (except the monzodiorite) plot in the volcanic arc field or the volcanic arc and sys-collisional field (Fig. 9). Additionally, the negative anomalies in Nb, Ta, P and Ti and the only in part slightly positive Eu anomalies (Fig. 6) suggest a subduction process during or before the formation of the diorites and hornblende granites in a continental arc setting, whereas the positive Rb, Th and La anomalies of some granitoids may be explained by the involvement of crustal melts (Wang et al. 2006). The slight Nb enrichment shown by the Monzodiorites may be due to the melting of a mantle source metasomatized by a slab-derived Nb-rich aqueous fluid (e.g. Sajona et al. 1996; Gao et al. 2007). Consequently, the petrographic and geochemical features favor a continental arc setting for the granitoids, which are exposed along the Kekesu River and Bikai River across the Central Tianshan Terrane.

Timing of magmatism

The U–Pb zircon ages obtained for the different granitoids are considered to reflect the time of their emplacement due to the magmatic texture of the analyzed zircons. These ages indicate that magmatism of the Central Tianshan continental arc started about 480 Ma ago, culminating during two periods between 433–398 Ma and 352–349 Ma, and ending at about 275 Ma. This is supported by a comparison (Fig. 10) between the age data presented here and previously published U–Pb zircon ages for granitoids of the Central Tianshan Terrane, which suggests that the granitic magmatism originated in the early Ordovician (about 480 Ma), continued during the whole Palaeozoic from 460 to 320 Ma and ended at the end of the Palaeozoic (about 270 Ma) [for isotopic data, see Bureau of Geology and Mineral Resources of Xinjiang Uygur Autonomous Region (BGMXJ) 1993; Han et al. 2004; Gao et al. 2006; Xu et al. 2006; Yang et al. 2006; Zhu et al. 2006b; Long 2007; Shi et al. 2007]. In addition, a U–Pb age of 1,086 Ma for the inherited zircon (Sample BK14) and a U–Pb age of about 900 Ma, which was obtained on zircons from the granitic gneisses of the Central Tianshan Arc along the Duku Road (Chen et al. 2000b), confirm that a Neoproterozoic basement existed in the Central Tianshan Arc.

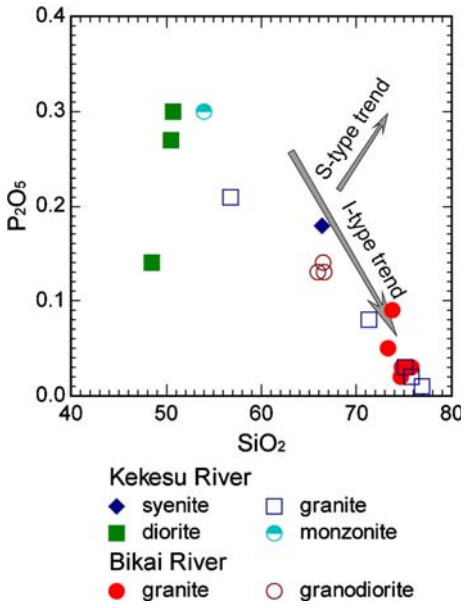

Fig. 8 P_2O_5 versus SiO_2 diagram for granitoids, showing the variation of P_2O_5 as a function of SiO_2-content for I- and S-type granites (after Chappell and White 1992)

Implications for the tectonic evolution of the South Tianshan orogen

Both the geochronological and geochemical data of the investigated granitoids in conjunction with recently published data for ophiolites, HP-LT metamorphic rocks and granites of Kyrgyzstan, Kazakhstan and China suggest a new tectonic model for the South Tianshan orogen and adjacent regions (Fig. 11).

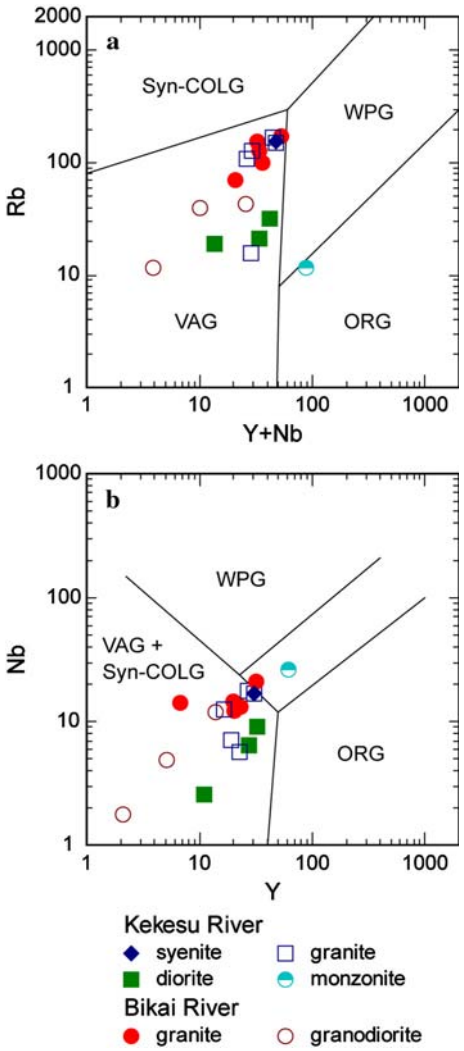

Fig. 9 Tectonic discrimination diagrams for granitoids (Pearce et al. 1984): **a** Y + Nb versus Rb; **b** Y versus Nb

The Neoproterozoic 'Xinjiang Craton' was formed in a subduction environment as is implied by the ca. 900 Ma Aksu blueschists and granitic gneisses of ca. 900 Ma (Nakajima et al. 1990; Wang et al. 1990; Xiao et al. 1992; Che et al. 1994; Chen et al. 2000b). Late Sinian (about 800 Ma) tillites occurring widespread in the northern margin of the Tarim plate, the north and south of the Yili plate and the Kazakhstan plate (Wang et al. 1990; Mikolaichuk et al. 1997) indicate that the Kazakhstan (North Tien Shan)–Yili, the Central Tianshan and Tarim plates were part of the 'Rodinia supercontinent' throughout the latest Proterozoic (Xu et al. 2005). The U–Pb age of 755 ± 15 Ma, which was derived from zircons from volcanic rocks of the Beiyixi Formation in northwestern Tarim (Xu et al. 2005), may indicate the breakup of the 'Xinjiang Craton' during the separation from Rodinia.

The 'Terskey Ocean,' which extends along the present 'Nikolaev Line,' may have formed and separated the Kazakhstan–Yili and Tarim plates from the latest Neo-Proterozoic to Early Ordovician (Fig. 11a; Lomize et al. 1997; Bazhenov et al. 2003; Qian et al. 2008). Mid-oceanic ridge basalts with a SHRIMP U–Pb zircon age of 516 Ma—occurring along the eastern extension of the 'Nikolaev Line' (Qian et al. 2008)—confirmed the existence of the 'Terskey Ocean' between the Tarim–Central Tianshan and Yili plates (Fig. 11a). This Early Paleozoic Ocean may, respectively, to be the result of a simultaneous southward and northward subduction beneath the northern margin of the Tarim plate and the Kazakhstan–Yili plate, thereby creating two magmatic margins. The southern magmatic margin is represented by the ca. 480 Ma granitic pluton in the Bikai River (see above). The northern margin is represented by the 470–460 Ma granites in Kyrgyzstan (Kiselev 1999; Konopelko et al. 2008) and the Xiate

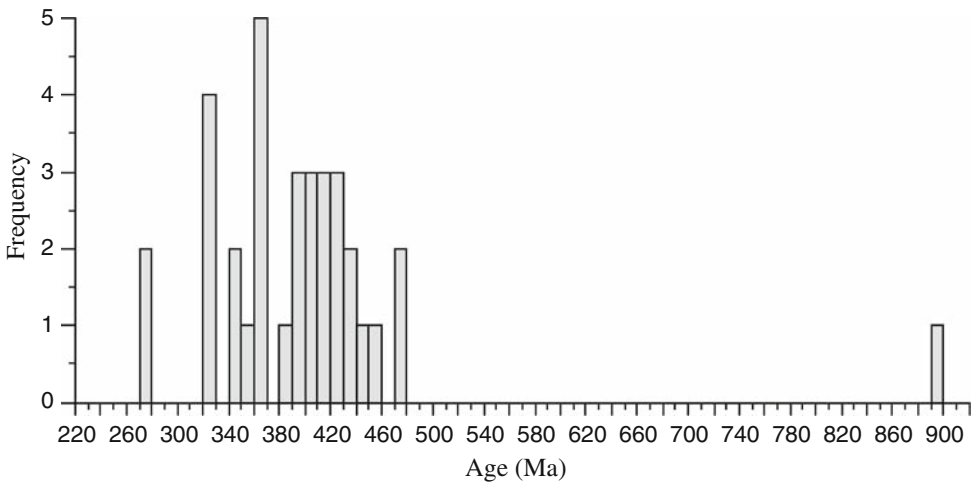

Fig. 10 Statistics of the zircon ages obtained for the granitoids intruding into the Central Tianshan Terrane. Data from this study; Bureau of Geology and Mineral Resources of Xinjiang Uygur Autonomous Region (BGMXJ) 1993; Han et al. 2004; Gao et al. 2006; Xu et al. 2006; Yang et al. 2006; Zhu et al. 2006b; Long 2007 and Shi et al. 2007

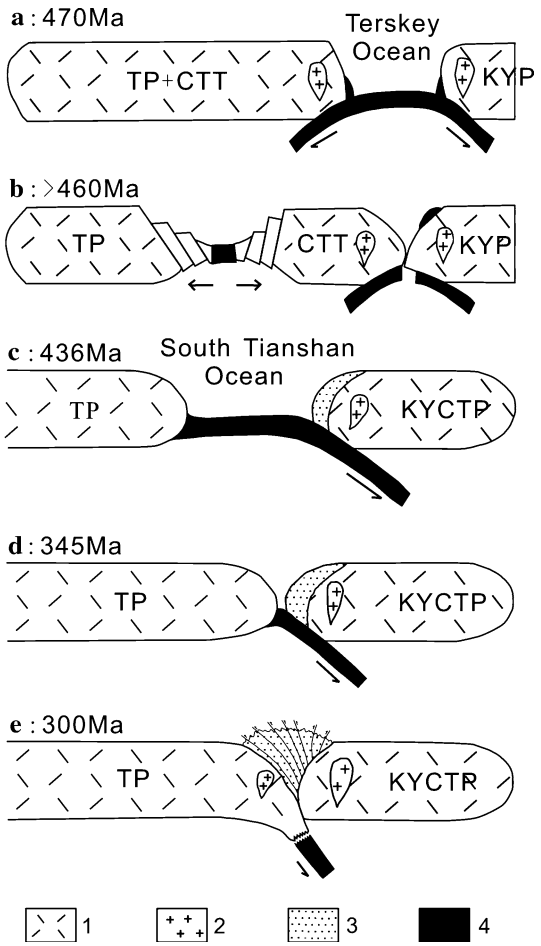

Fig. 11 Tectonic evolution model for the South Tianshan orogen. *1* continental crust, *2* granitic intrusions, *3* melange in the accretionary wedge, *4* oceanic crust. *TP* Tarim plate, *KYP* Kazakhstan–Yili plate, *CTT* Central Tianshan Terrane, *KYCTP* Kazakhstan–Yili–Central Tianshan plate

dioritic pluton with an age of about 470 Ma (Qian et al. 2008). The closure of the Terskey Ocean is considered to be related to the collision of the Kazakhstan–Yili and the Central Tianshan Terranes at the end of Middle Ordovician (Fig. 11b; Lomize et al. 1997; Bazhenov et al. 2003; Qian et al. 2008; Long 2007).

The 'South Tianshan Ocean' gradually originated in response to the subduction of the Terskey Ocean to the south, thereby separating the northern margin (the Central Tianshan Terrane) from the Tarim plate. Consequently, the Central Tianshan Terrane formed the southern margin of the amalgamated Kazakhstan–Yili–Central Tianshan plate (Fig. 11c). U–Pb zircon ages of about 450 Ma for oceanic island basalts (Wang et al. 2007c) and about 425 Ma for mid-oceanic ridge basalts (Long et al. 2006) are interpreted to represent the initiation point of the South Tianshan Ocean. It is suggested that this ocean was subducted toward the north beneath the southern margin of the Kazakhstan–Yili–Central Tianshan plate (Fig. 11c, d; Windley et al. 1990; Allen et al. 1992; Gao et al. 1998; Chen et al. 1999a; Gao and Klemd 2003; Gao et al. 2006). The granitic magmatism of this period, which culminated between 460 and 320 Ma, was initiated by the subduction process.

However, the point of closure of the South Tianshan Ocean and of collision between the Tarim and the Kazakhstan–Yili–Central Tianshan plates are still being controversially discussed. Some authors have suggested a Late Paleozoic age (e.g. Allen et al. 1992; Gao et al. 1998, 2006; Gao and Klemd 2003; Charvet et al. 2007; Solomovich 2007; Wang et al. 2007b; Jong et al. 2008; Li et al. 2008), whereas others have proposed a Triassic collision age (e.g. Li et al. 2002; Zhang et al. 2007a, b; Xiao et al. 2008). The geochronological data obtained in this study support a complete eradication of the South Tianshan Ocean in Late Carboniferous times, and a subsequent collision of the Tarim and Kazakhstan–Yili–Central Tianshan plates along the South Central Tianshan suture zone (Fig. 11e; Gao et al. 1998). The Sm–Nd isochron (omp–gln–grt–wr) of 343 ± 44 Ma for the eclogites, $^{40}Ar/^{39}Ar$ ages of 340–345 Ma for glaucophane and the $^{40}Ar/^{39}Ar$ and Rb–Sr white mica ages of 335–310 Ma of the western Tianshan HP–LT metamorphic belt in NW China (Gao and Klemd 2003; Gao et al. 2006; Klemd et al. 2005) and the $^{40}Ar/^{39}Ar$ plateau ages of 327–324 Ma for phengites of the Atbashy eclogites in Kyrgyzstan (Stupakov et al. 2004) confirm a late Carboniferous collision. The postcollisional syenites, nephelite syenites, aegirine syenites, two-mica peraluminous leucogranites and A-type rapakivi granites with ages varying from 296 to 269 Ma (Solomovich and Trifonov 2002; Mao et al. 2004; Liu et al. 2004; Konopelko et al. 2007; Wang et al. 2007c; Long et al. 2008) extensively intruded in Paleozoic sedimentary strata in the South Tianshan, indicating that the collision between the Tarim and the Kazakhstan–Yili–Central Tianshan plates must have started at the beginning of Early Permian. The 275 Ma syenite reported in this paper may also represent a postcollisional intrusion event, which was superimposed on the earlier continental arc setting of the Central Tianshan. The Upper Permian continental molasse, which was deposited in the Kuche basin, adjacent to the southern margin of the South Tianshan orogen, further constrains the timing of the collision to be pre-Permian (Zhu et al. 1999; Lu et al. 2001). The paleomagmatic data also indicate that the North Tien Shan (Kazakhstan–Yili–Central Tianshan plate), Siberian and Tarim plates were amalgamated at about 300 Ma (Bazhenov et al. 2003). The clockwise rotation of the Tarim block is interpreted to have created the large-scale strike-slip movement between the Yili and Tarim blocks in Early Permian times (Wang et al. 2007a). This Permian movement is in agreement with the timing of other transcurrent faults in the Tianshan orogen

and adjacent regions (Shu et al. 1999; Laurent-Charvet et al. 2002, 2003; Charvet et al. 2007; Jong et al. 2008).

A Triassic collisional time is based on younger U–Pb ages of 233–226 Ma obtained on zircons from the western Tianshan eclogites in China (Zhang et al. 2007a; Xiao et al. 2008) and one Late Permian Radiolaria fossil found in the cherts, which are interlayered with volcanic in Kokshal of the South Tianshan (Li et al. 2002). However, the zircon rim age of 233–226 Ma is interpreted to be due to the fluid-mediated recrystallization of zircons (Jong et al. 2008). A U–Pb age of 291 Ma obtained on zircons from the western Tianshan rodingites, which are greenschist-facies retrograde products of former eclogites (Li et al. 2005b, 2007), further indicate that the Triassic ages for eclogites cannot be related to the collision of the Tarim and Yili–Central Tianshan plates. In addition, Early Carboniferous Conodonts, such as *Hindeodella* sp., *Ozarkodina* sp. and *Hindeodus* sp., have also been reported recently from the same locality where the Late Permian Radiolaria was found (Wang et al. 2007c). The Permian postcollisional shoshonitic volcanic and their shallow level plutonic counterparts, which are widely distributed in the North Tien Shan of Kyrgyzstan (Solomovich 2007) and the Yili block of China (Zhao et al. 2003), further show that the collision between the Tarim and Kazakhstan–Yili–Central Tianshan plates must have occurred during the Carboniferous and not Triassic time. Furthermore, the orogenic evolution in central Kazakhstan, southern Kazakhstan and southern Mongolia was also terminated in Permian times indicating that the whole Central Asia orogenic belt is a Paleozoic orogenic belt (Kröner et al. 2007, 2008).

Conclusions

1. The petrological and geochemical data obtained for the granitoids from the Kekesu River and the Bikai River indicate that the granitic plutons intruded into a continental arc setting, the Central Tianshan Terrane.
2. The SHRIMP and La-ICP-MS U–Pb zircon ages derived for the granitoids indicate that magmatism started at about 479 Ma, continued from 460 to 330 Ma and ended at about 275 Ma.
3. The earlier phase of magmatism (>470 Ma) is considered to be related to the southward subduction of the Terskey Ocean beneath the northern margin of the Tarim plate. The closure of the Terskey Ocean induced the collision of the Kazakhstan (North Tien Shan)–Yili and the Central Tianshan Terrane and the separation of the Central Tianshan Terrane from the Tarim plate in late Ordovician.
4. The later phase of magmatism (460–330 Ma) corresponds with the the northward subduction of the South Tianshan Ocean beneath the southern margin of the Kazakhstan (North Tien Shan)–Yili–Central Tianshan plate. The collision of the Tarim and the Kazakhstan–Yili–Central Tianshan plates occurred in Later Carboniferous time.
5. The South Tianshan orogen is a Late Paleozoic collisional orogenic belt, not a Triassic one.

Acknowledgments This research was supported by 'National Basic Research Program of China' (Nos. 2007CB411302 and 2007CB411304), National Natural Science Foundation of China (40672153, 40721062 and 40872057), and the Deutsche Forschungsgemeinschaft (KL 692/17-2). We are indebted to J. Q. Wang for conducting the XRF-analyses, X. D. Jin and H. Y. Li for their arrangement in the trace element analysis, B. Song and H. Tao for help during the SHRIMP dating and X. M. Liu for help during the La-ICP-MS dating. We thank Mr. Y. G. Ma and Q. Mao for their help with the Cathodoluminescence (CL) images. Constructive reviews by M. Sun and an anonymous reviewer are highly appreciated.

References

Ai YL, Zhang LF, Li XP, Qu JF (2005) The geochemistry characters of the HP-UHP eclogites and blueschist and its tectonic significance, Southwestern Tianshan, Xinjiang. Prog Nat Sci 15:1346–1356

Allen MB, Windley BF, Zhang C (1992) Palaeozoic collisional tectonics and magmatism of the Chinese Tien Shan, central Asia. Tectonophysics 220:89–115. doi:10.1016/0040-1951(93)90225-9

Bazhenov ML, Collins AQ, Degtyarev KE, Levashova NM, Mikolaichuk AV, Pavlov VE et al (2003) Paleozoic northward drift of the North Tien Shan (Central Asia) as revealed by Ordovician and Carboniferous paleomagnetism. Tectonophysics 366: 113–141. doi:10.1016/S0040-1951(03)00075-1

Black LP, Kamo SL, Allen CM, Aleinikoff JN, Davis DW, Korsch RJ et al (2003) TEMORA 1: a new zircon standard for Phanerozoic U–Pb geochronology. Chem Geol 200:155–170. doi:10.1016/S0009-2541(03)00165-7

Brookfield ME (2000) Geological development and Phanerozoic crustal accretion in the western segment of the southern Tien Shan (Kyrgyzstan, Uzbekistan and Tagikistan). Tectonophysics 328:1–14. doi:10.1016/S0040-1951(00)00175-X

Bureau of Geology and Mineral Resources of Xinjiang Uygur Autonomous Region (BGMXJ) (1993) Regional geology of Xinjiang Uygur Autonomous Region. Geological Publishing House, Beijing, pp 390–566 (in Chinese with English abstract)

Burtman VS (1975) Structural geology of the Variscan Tien Shan, USSR. Am J Sci 272A:157–186

Carroll AR, Graham SA, Hendrix MS, Ying D, Zhou D (1995) Late Paleozoic tectonic amalgamation of northwestern China: sedimentary record of the north Tarim, northwestern Turpan and southern Junggar basins. Geol Soc Am Bull 107:571–594. doi:10.1130/0016-7606(1995)107<0571:LPTAON>2.3.CO;2

Chappell BW, White AJR (1992) I- and S-type granites in the Lachlan Fold Belt. Trans R Soc Edinb Earth Sci 83:1–26

Charvet J, Shu LS, Laurent-Charvet S (2007) Paleozoic structural and geodynamic evolution of eastern Tianshan (NW China): welding of the Tarim amd Junggar plates. Episodes 30:162–186

Che ZC, Liu HF, Liu L (1994) Formation and evolution of the middle Tianshan orogenic belt. Geological Publishing House, Beijing, pp 1–135 (in Chinese with English abstract)

Chen B, Jahn BM (2004) Genesis of post-collisional granitoids and basement nature of the Junggar Terrane, NW China: Nd–Sr isotope and trace element evidence. J Asian Earth Sci 23:691–703. doi:10.1016/S1367-9120(03)00118-4

Chen C, Lu F, Jia D, Cai D, Wu S (1999a) Closing history of the southern Tianshan oceanic basin, Western China: an oblique collisional orogeny. Tectonophysics 302:23–40. doi:10.1016/S0040-1951(98)00273-X

Chen YB, Hu AQ, Zhang GX (1999b) Zircon U–Pb age and Nd–Sr isotopic composition of granitic gneiss and its geological implications from Precambrian tectonic window of western Tianshan, NW China. Geochemica 28(6):515–520 (in Chinese with English abstract)

Chen YB, Hu AQ, Zhang GX (2000a) Precambrian basement age and characteristics of Southwestern Tianshan: Zircon U–Pb geochronology and Nd–Sr isotopic compositions. Acta Petrol Sin 16(1):91–98 (in Chinese with English abstract)

Chen YB, Hu AQ, Zhang GX, Zhang QF (2000b) Zircon U–Pb age of granitic gneiss on Duku highway in western Tianshan of China and its geological implications. Chin Sci Bull 45(7):649–653. doi:10.1007/BF02886044

Coleman RG (1989) Continental growth of northwest China. Tectonics 8:621–635. doi:10.1029/TC008i003p00621

Dobretsov NL, Coleman RG, Liou G, Maruyama S (1987) Blueschist belts in Asia and possible periodicity of blueschist facies metamorphism. Ofioliti 12:445–456

Gao J, Klemd R (2001) Primary fluids entrapped at blueschist to eclogite transition: evidence from the Tianshan meta-subduction complex in northwestern China. Contrib Mineral Petrol 142: 1–14

Gao J, Klemd R (2003) Formation of HP-LT rocks and their tectonic implications in the western Tianshan Orogen, NW China: geochemical and age constraints. Lithos 66:1–22. doi:10.1016/S0024-4937(02)00153-6

Gao J, Xiao XC, Tang YQ, Zhao M, Wang J, Wu HQ (1993) The discovery of blueschist in Kumux of the South Tianshan Mountains and its tectonic significance. Reg Geol China (4):344–347 (in Chinese with English abstract)

Gao J, He G, Li M, Tang Y, Xiao X, Zhou M et al (1995) The mineralogy, petrology, metamorphic PTDt trajectory and exhumation mechanism of blueschists, South Tianshan, northwestern China. Tectonophysics 250:151–168. doi:10.1016/0040-1951(95)00026-6

Gao J, Li M, Xiao X, Tang Y, He G (1998) Paleozoic tectonic evolution of the Tianshan orogen, northwestern China. Tectonophysics 287:213–231. doi:10.1016/S0040-1951(97)00211-4

Gao J, Klemd R, Zhang L, Wang Z, Xiao X (1999) P–T path of high pressure–low temperature rocks and tectonic implications in the western Tianshan Mountains (NW China). J Metamorph Geol 17:621–636. doi:10.1046/j.1525-1314.1999.00219.x

Gao J, Zhang LF, Liu SW (2000) The $^{40}Ar/^{39}Ar$ age record of formation and uplift of the blueschists and eclogites in the western Tianshan Mountains. Chin Sci Bull 45:1047–1052. doi:10.1007/BF02884989

Gao J, Xiao W, Li J, Han B, Guo Z, Wang J (2002) 'Central-Asia type' Orogenesis and Metallogenesis in western China. IGCP 420 Project workshop (abstract), Changchun, China, August 5–14, p 39

Gao J, Long LL, Qian Q, Huang DZ, Su W, Klemd R (2006) South Tianshan: a late Paleozoic or a Triassic Orogen. Acta Petrol Sin 22(5):1049–1061 (in Chinese with English abstract)

Gao J, Klemd R, John T, Xiong X (2007) Mobilisation of Ti–Nb–Ta during subduction: evidence from rutile-bearing segregations and veins hosted in eclogites, Tianshan, NW China. Geochim Cosmochim Acta 71:4974–4996. doi:10.1016/j.gca.2007.07.027

Ges MD, Garetskaya EN, Izraileva RM, Leskov SA (1982) Permian intrusive rocks. In: Osmonbetov KO, Knauf VI, Korolev VG (eds) Stratified and Intrusive Formations of Kyrgyzia. Ilim Press, Frunze, pp 128–181 (in Russian)

Guo ZJ, Ma RS, Guo LZ, Shi YS (1993) A comparative study on three ophiolitic melange belts in eastern Xinjiang. Geol Rev 39(3):236–247 (in Chinese with English abstract)

Han B, Wang S, Jahn BM, Hong D, Kagami H, Sun Y (1997) Depleted-mantle source for the Ulungur River A-Type granites from North Xinjiang, Chian: geochemistry and Nd–Sr isotopic evidence, and implications for Phanerozoic crustal growth. Chem Geol 138:135–159. doi:10.1016/S0009-2541(97)00003-X

Han BF, He GQ, Wu TR, Li HM (2004) Zircon U–Pb dating and geochemical features of early Paleozoic granites from Tianshan, Xinjiang: implications for tectonic evolution. Xinjiang Geol 22(1):4–11 (in Chinese with English abstract)

He GQ, Li MS (2000) New achievement in researching ophiolitic belts in central Asia and its significance in the links of tectonic belts between northern Xinjiang and adjacent area. Xinjiang Geol 18:193–202 (in Chinese with English abstract)

He GQ, Li MS, Han BF (2001) Geotectonic research of southwest Tianshan and its west adjacent area, China. Xinjiang Geol 19(1):7–11 (in Chinese with English abstract)

Hendrix MS, Dumitru TA, Graham SA (1994) Late Oligocene-early Miocene unroofing in the Chinese Tian Shan: an early effect of the India–Asia collision. Geology 22:487–490. doi:10.1130/0091-7613(1994)022<0487:LOEMUI>2.3.CO;2

Heubeck C (2001) Assembly of central Asia during the middle and late Paleozoic. In: Hendrix MS, Davis GA (eds) Paleozoic and Mesozoic tectonic evolution of central Asia: from continental assembly to intracontinental deformation. Geological Society of America Memoir 194. Geological Society of America, Boulder, pp 1–22

Hopson C, Wen J, Tilton G, Tang Y, Zhu B, Zhao M (1989) Paleozoic plutonism in East Junggar, Bogdashan, and eastern Tianshan, NW China. Eos Trans AGU 70:1403–1404

Huang TK, Ren JS, Jiang CF, Zhang ZM, Qian DY (1987) Geotectonic evolution of China. Springer, New York, p 203

Institute of Geology of Chinese Academy of Geological Sciences (IGCAGS) (2006) 1:2,500,000 Geological Map of the Western China and adjacent regions. Geological Publishing House, Beijing (in Chinese)

Jahn BM (2004) Phanerozoic continental growth in Central Asia. J Asian Earth Sci 23:599–603. doi:10.1016/S1367-9120(03)00124-X

Jahn BM, Griffin WL, Windley BF (2000a) Continental growth in the Phanerozoic: evidence from Central Asia. Tectonophysics 328:vii–x. doi:10.1016/S0040-1951(00)00174-8

Jahn BM, Wu F, Chen B (2000b) Granitoids of the Central Asian orogenic belt and continental growth in the Phanerozoic. Trans R Soc Edinb Earth Sci 91:181–193

Jiang CY, Mu YM, Bai KY (1999) Chronology, petrology, geochemistry and tectonic environment in the southern Tianshan Mountain, western China. Acta Petrol Sin 15(2):298–308 (in Chinese with English abstract)

John T, Klemd R, Gao J, Garbe-Schönberg CD (2008) Trace element mobilization in slabs due to non steady-state fluid–rock interaction: constraints from an eclogite-facies transport vein in blueschist (Tianshan, China). Lithos 103:1–24. doi:10.1016/j.lithos.2007.09.005

Jong KD, Wang B, Faure M, Shu L, Cluzel D, Charvet J, et al (2008) New 40Ar/39Ar age constraints on the Late Paleozoic tectonic evolution of the western Tianshan (Xinjiang, northwestern China), with emphasis on Permian fluid ingress. Int J Earth Sci (this issue)

Khain VE (1985) Geology of USSR. Gebruder Borntraeger, Berlin, pp 1–272

Kiselev VV (1999) The U–Pb (by zircons) geochronology of magmatic suits of the Northern Tien Shan. In: Bakirov AB, Dikikl AN (eds) Problems of geology and geography in Kyrgystan (Proceedings of the National Academy of Sciences of Kyrgyz Republic). Ilim, Bishkek, pp 21–33 (in Russian)

Klemd R (2003) Ultrahigh-pressure metamorphism in eclogites from the western Tianshan high-pressure belt (Xinjiang, western China)—comment. Am Mineral 88:1153–1156

Klemd R, Schröter FC, Will TM, Gao J (2002) PT-evolution of glaucophane-omphacite bearing HP-LT rocks in the western Tianshan orogen, NW China: new evidence for 'Alpine-type' tectonics. J Metamorph Geol 20:239–254. doi:10.1046/j.1525-1314.2002.00347.x

Klemd R, Bröcker M, Hacker BR, Gao J, Gans P, Wemmer K (2005) New age constraints on the metamorphic evolution of the high-pressure/low-temperature belt in the western Tianshan Mountains, NW China. J Geol 113:157–168. doi:10.1086/427666

Konopelko D, Biske G, Seltmann R, Eklun O, Belyatsky B (2007) Hercynian post-collisional A-type granites of the Kokshaal Range, Southern Tien Shan. Lithos 97:140–160. doi:10.1016/j.lithos.2006.12.005

Konopelko D, Biske G, Seltmann R, Kiseleva M, Matukov D, Sergeev S (2008) Deciphering Caledonian events: timing and geochemistry of the Caledonian magmatic arc in the Kyrgyz Tien Shan. J Asian Earth Sci 32:131–141

Kröner A, Windley BF, Badarch G, Tomurtogoo O, Hegner E, Jahn BM, et al (2007) Accretionary growth and crust formation in the Central Asian Orogenic Belt and comparison with the Arabian-Nubian shield. In: Hatcher RD, Carlson MP, McBride JH, Martínez Catalán JR (eds) 4-D framework of continental crust. Geological Society of America Memoir 200. Geological Society of America, Boulder, pp 181–209

Kröner A, Hegner E, Lehmann B, Heinhorst J, Wingate MTD, Liu DY, Ermelov P (2008) Palaeozoic arc magmatism in the Central Asian Orogenic Belt of Kazakhstan: SHRIMP zircon ages and whole-rock Nd isotopic systematic. J Asian Earth Sci 32:118–130

Laurent-Charvet S, Charvet J, Shu LS, Ma RS, Lu HF (2002) Paleozoic late collisional strike-slip deformations in Tianshan and Altay, Eastern Xinjinag, NW China. Terra Nova 14:249–256. doi:10.1046/j.1365-3121.2002.00417.x

Laurent-Charvet S, Charvet J, Monie' P, Shu LS (2003) Late Paleozoic strike-slip shear zones in eastern central Asia (NW China): new structural and geochronological data. Tectonics 22:1099–1101. doi:10.1029/2001TC901047

Li XD, Li MS (1997) Tectonic correlation between the western Chinese Tianshan and its western adjacent area. Geol Rev 42:107–115 (in Chinese with English abstract)

Li CY, Wang Q, Liu XY, Tang YQ (1982) 1:8, 000, 000 tectonic map of Asia. Cartographic Publisher House, Beijing

Li YJ, Wang ZM, Wu HR, Huang ZB, Tan ZJ, Luo JC (2002) Discovery of Radiolarian fossils from the Aketik group at the western end of South Tianshan Mountains of China and its implications. Acta Geol Sin 76(2):146–154

Li YJ, Sun LD, Wu HR, Wang GL, Yang CS, Peng GX (2005a) Permo-Carboniferous radiolarian from the Wupatarkan Group, west terminal of Chinese South Tianshan. Sci Geol Sin 40(2):220–226 (in Chinese with English abstract)

Li XP, Zhang LF, Ai YL, Qu JF, Song B, Liu XM (2005b) Zircons from the rodingite of serpentinite complex, Western Tianshan: mineral chemistry and U–Pb ages. Abstract presented at the 2005 national petrological and geodynamic conference, Hangzhou, November 14–20, p 397

Li JY, He GQ, Xu X, Li HQ, Sun GH, Yang TN et al (2006) Crustal tectonic framework of northern Tianshan and adjacent regions and its formation. Acta Geol Sin 80(1):149–168 (in Chinese with English abstract)

Li XP, Zhang LF, Wei V, Ai Y, Chen J (2007) Petrology of rodingite derived from eclogite in western Tianshan, China. J Metamorph Geol 25:363–382. doi:10.1111/j.1525-1314.2007.00700.x

Li XG, Liu SW, Wang ZQ, Han BF, Shu GM, Wang T (2008) Electron microprobe monazite geochronological constraints on the Late Palaeozoic tectonothermal evolution in the Chinese Tianshan. J Geol Soc London 165:511–522. doi:10.1144/0016-76492007-077

Liao Ning Institute of Geological Survey (LNIGS) (2005) Geological map of the Akesu region, scale 1:50000, Explanation. Urimqi, pp 1–175 (in Chinese)

Lin W, Enami M (2006) Prograde pressure–temperature path of jadeite-bearing eclogites and associated high-pressure/low-temperature rocks from western Tianshan, northwest China. Isl Arc 15:483–502. doi:10.1111/j.1440-1738.2006.00545.x

Liu Y (2001) Early Carbonferous Radiolarian Fauna from Heiyingshan, south of the Tianshan Mountains and its geotectonic significance. Acta Geol Sin 75(1):101–108

Liu B, Qian YX (2003) The geologic characteristics and fluid evolution in the three high-pressure metamorphic belts of eastern Tianshan. Acta Petrol Sin 19(2):283–292 (in Chinese with English abstract)

Liu Y, Hao SG (2006) Evolutionary significance of Pylentonemid Radiolarians and their Late Devonian species from southwestern Tianshan, China. Acta Geol Sin 80(5):647–655

Liu YM, Yang WH, Gai JY (1994) Study on isotopic age of Dahalajunshan formation in Tekesi forestry of Xinjing. Geochimica 23:99–104

Liu CX, Xu BL, Zhou TR (2004) Petrochemistry and tectonic significance of Hercynian alkaline rocks along the northern margin of the Tarim platform and its adjacent area. Xinjiang Geol 22(1):43–49 (in Chinese with English abstract)

Lomize MG, Demina LI, Zarshchicov AV (1997) The Kyrgyz–Terskei paleoceanic basin in the Tien Shan. Geotectonics 31(6):463–482 (in Russian with English abstract)

Long LL (2007) Paleozoic tectonic evolution and continental growth of the West Tianshan Orogen: evidence from granitoids and ophiolites. Doctoral dissertation, Chinese Academy of Sciences, Beijing, pp 1–163 (in Chinese with English abstract)

Long LL, Gao J, Xiong XM, Qian Q (2006) The geochemical characteristics and the age of the Kule Lake ophiolite in the southern Tianshan. Acta Petrol Sin 22(1):65–73 (in Chinese with English abstract)

Long LL, Gao J, Qian Q, Xiong XM, Wang JB, Wang YW et al (2008) Geochemistry and SHRIMP Zircon U–Pb age of post-collisional granites in the Southwest Tianshan Orogenic Belt of China: examples from the Heiyingshan and Laohutai plutons. Acta Geol Sin 82(2):415–424

Lu HF, Jia CZ, Jia D (2001) Features of the thrust wedge of deformation belt in Kuqa rejuvenation foreland basin. Geol J China Univ 7(3):257–271 (in Chinese with English abstract)

Ludwig KR (1991) Isoplot: A plotting and regression program for radiogenic-isotope data, version 2.0. US Geological Survey open-file report, p 39

Ma RS, Wang CY, Ye SF (1993) Tectonic framework and crustal evolutional of Eastern Tianshan mountains. Publishing House of Nanjing University, Nanjing, pp 1–225 (in Chinese with English abstract)

Ma RS, Shu LS, Sun JQ (1997) Tectonic evolution and metallogeny of Eastern Tianshan mountains. Geological Publishing House, Beijing, pp 1–202 (in Chinese with English abstract)

Maniar PD, Piccoli PM (1989) Tectonic discrimination of granitoids. Geol Soc Am Bull 101:635–643. doi:10.1130/0016-7606(1989)101<0635:TDOG>2.3.CO;2

Mao JW, Konopelko D, Seltmann R, Lehmann B, Chen W, Wang YT et al (2004) Postcollisional age of the Kumtor gold deposit and timing of Hercynian events in the Tien Shan, Kyrgyzstan. Econ Geol 99:1771–1780. doi:10.2113/99.8.1771

Middlemost EAK (1994) Naming materials in the magma/igneous rocks system. Earth Sci Rev 37:215–224. doi:10.1016/0012-8252(94)90029-9

Mikolaichuk AV, Kotov VV, Kuzikov SI (1995) The structural position of the Malyi Naryn metamorphic complex and boundary between the North and Middle Tien Shan. Geotectonics 29(2):157–166

Mikolaichuk AV, Kurenkov SA, Degtyarev KE, Rubtsov VI (1997) Main stages of geodynamic evolution of the North Tien Shan in the late Precambian and early Paleozoic. Geotectonics 31(6):16–34

Milanovsky EE (1996) Geology of Russia and adjacent domain. Publishing House of MGU, Moscow, pp 1–445 (in Russian)

Nakajima T, Maruyama S, Uchiumi S, Liou JG, Wang XZ, Xiao XC et al (1990) Evidence for Late Proterozoic subduction from 700-Myr-old blueschists in China. Nature 346:263–265. doi:10.1038/346263a0

Pearce JA, Harris NBW, Tindle AG (1984) Trace element discrimination diagrams for the tectonic interpretation of granitic rocks. J Petrol 25:956–983

Peccerillo R, Taylor SR (1976) Geochemistry of Eocene calc-alkaline volcanic rocks from the Kastamonu area, northern Turkey. Contrib Mineral Petrol 58:63–81. doi:10.1007/BF00384745

Qian Q, Gao J, Xiong XM, Huang DZ, Long LL (2006) Petrogenesis and tectonic settings of Carboniferous volcanic rocks from north Zhaosu, western Tianshan Mountains: constraints from petrology and geochemistry. Acta Petrol Sin 22:1307–1323 (in Chinese with English abstract)

Qian Q, Gao J, Klemd R, He G, Xiong XM, Long LL, et al (2008) Early Paleozoic tectonic evolution of the Chinese South Tianshan Orogen: constraints from SHRIMP zircon U–Pb geochronology and geochemistry of basaltic and dioritic rocks from Xiate, NW China. Int J Earth Sci (in press). doi:10.1007/s00531-007-0268-x

Sajona FG, Maury RC, Bellon H, Votten J, Defant M (1996) High field strength element enrichment of Pliocene-Pleistocene Island arc basalts, Zamboanga Peninsula, Western Mindanao (Philippines). J Petrol 37:693–726. doi:10.1093/petrology/37.3.693

Sengör AMC, Natal'In BA, Burtman VS (1993) Evolution of the Altaid tectonic collage and Paleozoic crustal growth in Eurasia. Nature 364:299–307. doi:10.1038/364299a0

Shi Y, Lu H, Jia D, Cai D, Wu S, Chen C et al (1994) Paleozoic plate-tectonic evolution of Tarim and Western Tianshan regions, Western China. Int Geol Rev 36:1058–1066

Shi YR, Liu DY, Zhang Q, Jian P, Zhang FQ, Miao LC (2007) SHRIMP zircon U–Pb dating of the Gangou granitoids, Central Tianshan Mountains, Northwest China and tectonic significances. Chin Sci Bull 52:1507–1516. doi:10.1007/s11434-007-0204-2

Shu LS, Charvet J, Guo L, Lu H (1999) A large-scale Paleozoic dextral ductile strike-slip zone: the Aqqikkudug-Weiya zone along the northern margin of the Central Tianshan belt, Xinjiang, NW China. Acta Geol Sin 73(2):148–162

Shu LS, Yu JH, Charvet J, Laurent-Charvet S, Sang HQ, Zhang RG (2004) Geological, geochronnological and geochemical features of granulites in the eastern Tianshan, NW China. J Asian Earth Sci 20(3):583–594

Solomovich LI (2007) Postcollisional magmatism in the South Tien Shan Variscan orogenic belt, Kyrgyztan: evidence for high-temperature and high-pressure collision. J Asian Earth Sci 30:142–153. doi:10.1016/j.jseaes.2006.08.003

Solomovich LI, Trifonov BA (2002) Postcollisional granites in the South Tien Shan Variscan collisional belt, Kyrgyztan. J Asian Earth Sci 21:7–21. doi:10.1016/S1367-9120(02)00008-1

Stupakov SI, Volkova NI, Travin AV, Simonov A, Sakiev KS, Novgorodtsev OS (2004) Eclogites of Atbashi Ridge as indicators of Early Carboniferous collision in Southern Tien Shan. In: Chernyshov AI, Tishin PA, Bether OV, Vrublevsky VV, Gertner IF, Grinev OM, Krasnova TS (eds) Petrology of magmatic and metamorphic complexes. Issue 4, Tomsk Center for Scientific and Technical Information, pp 272–277 (in Russian)

Sun SS, McDonough WF (1989) Chemical and isotopic systematics of ocean basalts:implications for mantle composition and processes. In: Saunders AD, Norry MJ (eds) Magmatism in ocean basin. Geological Society of London Special Publication 42. Geological Society, London , pp 313–345

Tagiri M, Yano T, Bakirov A, Nakajima T, Uchiumi S (1995) Mineral parageneses and metamorphic P–T paths of ultrahigh-pressure eclogites from Kyrgyzstan Tien-Shan. Isl Arc 4:280–292. doi:10.1111/j.1440-1738.1995.tb00150.x

Wang ZX, Wu JY, Liu CH, Lu XC, Zhang JG (1990) Polycyclic tectonic evolution and metallogeny of the Tianshan Mountains. Science Press, Beijing, pp 1–217 (in Chinese with English abstract)

Wang BY, Lang ZJ, Li XD (1994) Study on the geological sections across the western segment of Tianshan Mountains, China. Science Press, Beijing, pp 1–202 (in Chinese)

Wang RS, Wang Y, Li HM (1998) Zircon U–Pb dating of Yushugou terrain of high-pressure granulite facies in Southern Tianshan Mountains and its geological significance. Chin J Geochem 27(6):517–523

Wang T, Hong DW, Jahn BM, Tong Y, Wang YB, Han BF et al (2006) Timing, petrogenesis and setting of Paleozoic synorogenic intrusions from the Altai Mountains, northwest China: implications for the tectonic evolution of an accretionary orogen. J Geol 114:735–751. doi:10.1086/507617

Wang B, Chen Y, Zhan S, Shu LS, Faure M, Cluzel D et al (2007a) Primary Carboniferous and Permian paleomagnetic results from the Yili Block (NW China) and their implications on the geodynamic evolution of Chinese Tianshan Belt. Earth Planet Sci Lett 263:288–308

Wang B, Shu LS, Cluzel D, Faure M, Charvet J (2007b) Geochemical constraints on Carboniferous volcanic rocks of Yili block (Xinjiang, NW China): implication for the tectonic evolution of Western Tianshan. J Asian Earth Sci 29:148–159. doi:10.1016/j.jseaes.2006.02.008

Wang C, Liu L, Luo JH, Che ZC, Teng ZH, Cao XD et al (2007c) Late Paleozoic post-collisional magmatism in the Southwestern Tianshan orogenic belt: an example from the Baleigong pluton in the Kokshal region. Acta Petrol Sin 23(8):1830–1840 (in Chinese with English abstract)

Wei CJ, Powell R, Zhang LF (2003) Eclogites from the south Tienshan, NW China: petrological characteristic and calculated mineral equilibria in the Na_2O–CaO–FeO–MgO–Al_2O_3–SiO_2–H_2O system. J Metamorph Geol 21:163–179. doi:10.1046/j.1525-1314.2003.00435.x

Wiedenbeck M, Alle P, Corfu F (1995) Three natural zircon standards for U–Th–Pb, Lu–Hf, trace element and REE analyses. Geostand Newsl 19:1–23. doi:10.1111/j.1751-908X.1995.tb00147.x

Windley BF, Allen MB, Zhang C, Zhao Z, Wang Q (1990) Paleozoic accretion and Cenozoic redeformation of the Chinese Tien Shan range, central Asia. Geology 18:128–131. doi:10.1130/0091-7613(1990)018<0128:PAACRO>2.3.CO;2

Windley BF, Alexeiev D, Xiao W, Kröner A, Badarch G (2007) Tectonic models for accretion of the Central Asian Orogenic

Belt. J Geol Soc London 164:31–47. doi:10.1144/0016-76492006-022

Wood DA, Joron JL, Treuil M, Norry M, Tarney J (1979) Elemental and Sr isotope variations in basic lavas from Iceland and the surrounding ocean floor. Contrib Mineral Petrol 70:3219–3339. doi:10.1007/BF00375360

Xia LQ, Xu XY, Xia ZC, Li XM, Ma ZP, Wang LS (2004) Petrogenesis of Carboniferous rift-related volcanic rocks in the Tianshan, northwestern China. Geol Soc Am Bull 116:419–433. doi:10.1130/B25243.1

Xiao XC, Tang YQ, Feng YM, Zhu BQ, Li JY, Zhao M (1992) Tectonic evolution of northern Xinjiang and its adjacent regions. Geological Publishing House, Beijing, pp 1–169 (in Chinese with English abstract)

Xiao WJ, Zhang LC, Qin KZ, Sun S, Li JL (2004) Paleozoic accretionary and collisional tectonics of the eastern Tianshan (CHINA): implications for the continental growth of Central Asia. Am J Sci 304:370–395. doi:10.2475/ajs.304.4.370

Xiao WJ, Han CM, Yuan C, Chen HL, Sun M, Lin SF et al (2006) The unique Carboniferous–early Permian tectonic-metallogenic framework of Northern Xinjiang (NW China): constraints for the tectonics of the southern Paleoasian Domain. Acta Petrol Sin 22(5):1062–1076 (in Chinese with English abstract)

Xiao WJ, Han CM, Yuan C, Sun M, Lin SF, Chen HL et al (2008) Middle Cambrian to Permian subduction-related accretionary orogenesis of Northern Xinjiang, NW China: implications for the tectonic evolution of central Asia. J Asian Earth Sci 32:102–117. doi:10.1016/j.jseaes.2007.10.008

Xu B, Jian P, Zheng HF, Zou HB, Zhang LF, Liu DY (2005) U–Pb zircon geochronology and geochemistry of Neoproterozoic volcanic rocks in the Tarim Block of northwest China: implications for the breakup of Rodinia supercontinent and Neoproterozoic glaciations. Precambrian Res 136:107–123. doi:10.1016/j.precamres.2004.09.007

Xu XY, Ma ZP, Xia ZC, Xia LQ, Li XM, Wang LS (2006) TIMS U–Pb isotopic dating and geochemical characteristics of Paleozoic granitic rocks from the Middle-Western section of Tianshan. Northeast Geol 39:50–75 (in Chinese with English abstract)

Yakubchuk A (2004) Architecture and mineral deposit settings of the Altaid orogenic collage: a revised model. J Asian Earth Sci 23:761–779. doi:10.1016/j.jseaes.2004.01.006

Yang TN, Li JY, Sun GH, Wang YB (2006) Earlier Devonian active continental arc in Central Tianshan: evidence of geochemical analyses and Zircon SHRIMP dating on mylonitized granitic rock. Acta Petrol Sin 22(1):41–48 (in Chinese with English abstract)

Yin A, Nie S, Craig P, Harrison TM, Ryerson FJ, Qian X et al (1998) Late Cenozoic tectonic evolution of the southern Chinese Tian Shan. Tectonics 17:1–27. doi:10.1029/97TC03140

Yuan HL, Wu FY, Gao S, Liu XM, Xu P, Sun DY (2003) Determination of U–Pb age and rare earth element concentrations of zircons from Cenozoic intrusions in northeastern China by Laser ablation ICP-MS. Chin Sci Bull 48(22):2411–2421

Zamaletdinov T (1994) Geodynamic map of the Kyrgyzstan, scale 1:500000, Explanation. Ilim Press, Bishkek, pp 1–50 (in Russian)

Zhai W, Sun XM, Gao J, He XP, Liang JL, Miao LC et al (2006) SHRIMP dating of zircons from volcanic host rocks of Dahalajunshan Formation in Axi gold deposit, Xinjiang, China, and its geological implications. Acta Petrol Sin 22(5):1399–1404 (in Chinese with English abstract)

Zhang LF, Ellis DJ, Jiang W (2002a) Ultrahigh pressure metamorphism in western Tianshan, China, part I: evidences from the inclusion of coesite pseudomorphs in garnet and quartz exsolution lamellae in omphacite in eclogites. Am Mineral 87:853–860

Zhang LF, Ellis DJ, Williams S, Jiang W (2002b) Ultrahigh pressure metamorphism in western Tianshan, China, part II: evidence from magnesite in eclogite. Am Mineral 87:861–866

Zhang LF, Ellis DJ, Williams S, Jiang W (2003) Ultrahigh pressure metamorphism in eclogites from the Western Tianshan, China—reply. Am Mineral 88:1157–1160

Zhang LF, Ai YL, Li Q (2005a) The formation and tectonic evolution of UHP metamorphic belt in southwestern Tianshan, Xinjiang. Acta Petrol Sin 21(4):1029–1038 (in Chinese with English abstract)

Zhang LF, Song SG, Liou JG, Li XP (2005b) Relict coesite exsolution in omphacite from Western Tianshan eclogites, China. Am Mineral 90:181–186. doi:10.2138/am.2005.1587

Zhang LF, Ai YL, Li XP, Rubatto D, Song B, Williams S et al (2007a) Triassic collision of western Tianshan orogenic belt, China: evidence from SHRIMP U–Pb dating of zircon from HP/UHP eclogitic rocks. Lithos 96:266–280. doi:10.1016/j.lithos.2006.09.012

Zhang LF, Ai YL, Song SG, Liou J, Wei CJ (2007b) A brief review of UHP meta-ophiolitic rocks, Southwestern Tianshan, Western China. Int Geol Rev 49:811–823. doi:10.2747/0020-6814.49.9.811

Zhao ZH, Bai ZH, Xiong XL, Mei HJ, Wang YX (2000) Geochemistry of alkali-rich igneous rocks of Northern Xinjiang and its implications for Geodynamics. Acta Geol Sin 74(2):321–328

Zhao ZH, Bai ZH, Xiong XL, Mei HJ, Wang YX (2003) $^{40}Ar/^{39}Ar$ chronological study of Late Paleozoic volcanic-hypabyssal igneous rocks in western Tianshan, Xinjiang. Geochimica 32(4):317–327 (in Chinese with English abstract)

Zheng JP, Griffin WL, O'Reilly SY, Zhang M, Liou JG, Pearson N (2006a) Granulite xenoliths and their zircons, Tuoyun, NW China: insight into Southwestern Tianshan lower crust. Precambrian Res 145:159–181. doi:10.1016/j.precamres.2005.12.001

Zheng JP, Griffin WL, O'Reilly SY, Zhang M, Pearson N, Luo ZH (2006b) The lithospheric mantle beneath the Southwestern Tianshan area. Contrib Mineral Petrol 151:457–479. doi:10.1007/s00410-006-0071-x

Zhou D, Graham SA, Chang EZ, Wang B, Hacker B (2001) Paleozoic tectonic amalgamation of the Chinese Tian Shan: evidence from a transect along the Dushanzi–Kuqa highway. In: Hendrix MS, Davis GA (eds) Paleozoic and Mesozoic tectonic evolution of central Asia: from continental assembly to intracontinental deformation. Geological Society of America Memoir 194. Geological Society of America, Boulder, pp 23–46

Zhou MF, Lesher CM, Yang ZX, Li JW, Sun M (2004) Geochemistry and petrogenesis of 270 Ma Ni–Cu–(PGE) sulfide-bearing mafic intrusions in the Huangshan district, Eastern Xinjiang, Northwestern China: implications for the tectonic evolution of the Central Asian orogenic belt. Chem Geol 209:233–257. doi:10.1016/j.chemgeo.2004.05.005

Zhu ZL, Gao SH, Liu ZZ (1999) West-South Tianshan mountain orogenic belt and foreland basin systems. Geoscience 13(3):275–280 (in Chinese with English abstract)

Zhu YF, Zhang LF, Gu LB, Guo X, Zhou J (2005) SHRIMP geochronologyand element geochemistry of Carboniferous volcanic rocks in the western Tianshan area. Chin Sci Bull 50(18):2004–2014

Zhu YF, Zhou J, Song B, Zhang LF, Guo X (2006a) Age of the "Dahalajunshan" formation in Xinjiang and its disintegration. Geol China 33(3):487–497 (in Chinese with English abstract)

Zhu ZX, Wang KZ, Zheng YJ (2006b) The Zircon SHRIMP dating of Silurian and Devonian granitic intrusions in the southern Yili Block, Xinjiang and preliminary discussion on their tectonic setting. Acta Petrol Sin 22(5):1193–1200 (in Chinese with English abstract)

Zonenshain LP, Kuzmin MI, Natapov LM (1990) Geology of the USSR: a plate-tectonic synthesis. In: Page BM (ed) American Geophysics Union, geodynamics Series 21. American Geophysics Union, Washington, DC, pp 1–242